Report
P-15-15
December 2016

KBS-3H

Geophysical logging of borehole KO8028F01

Karla Tiensuu
Eero Heikkinen

SVENSK KÄRNBRÄNSLEHANTERING AB

SWEDISH NUCLEAR FUEL
AND WASTE MANAGEMENT CO

Box 250, SE-101 24 Stockholm
Phone +46 8 459 84 00
skb.se

SVENSK KÄRNBRÄNSLEHANTERING

ISSN 1651-4416
SKB P-15-15
ID 1469504

December 2016

KBS-3H

Geophysical logging of borehole K08028F01

Karla Tiensuu, Suomen Malmi Oy

Eero Heikkinen, Pöyry Finland Oy

Keywords: Borehole geophysics, Borehole imaging, Äspö HRL.

This report concerns a study which was conducted for Svensk Kärnbränslehantering AB (SKB). The conclusions and viewpoints presented in the report are those of the authors. SKB may draw modified conclusions, based on additional literature sources and/or expert opinions.

Data in SKB's database can be changed for different reasons. Minor changes in SKB's database will not necessarily result in a revised report. Data revisions may also be presented as supplements, available at www.skb.se.

A pdf version of this document can be downloaded from www.skb.se.

© 2016 Svensk Kärnbränslehantering AB

Summary

Geophysical borehole logging was conducted in borehole K08028F01 in August 2014. The current work continued the method development that started with the measurements in borehole K03009F01 in February 2014. In the current work, geophysical borehole logging was for the first time conducted in Äspö HRL in a gently upward oriented borehole requiring water filling in the borehole. The survey program included the following methods: fluid temperature and electrical conductivity, normal resistivity and single point resistance (SPR), induced polarization (IP), focused resistivity, full waveform sonic, gamma-gamma density, natural gamma radiation, magnetic susceptibility, and acoustic imaging including caliper.

Lithological boundaries, fractures and saline groundwater flow were already seen from the first view of the data. Lithology, alteration and fracturing data from Boremap were used for length adjustment of data in this logging campaign. Raw logging data were computed to physical values using experimental ratios. Gamma-gamma density and magnetic susceptibility ratios were adjusted using petrophysical sample data from the same borehole. The resistivity and the P-wave velocities from the logging data were compared to petrophysical results.

The geophysical logging results indicated geophysical properties and their variability in the borehole indicating changes in lithology, fracturing and presence of more significant fractures (including potential “large fractures”). Gamma-gamma density, natural gamma radiation and susceptibility, and partly the velocities from the sonic logging data describe the lithological variation. Main rock types show different density levels. Susceptibility is generally high due to elevated magnetite content. Density and susceptibility are lowest in intervals in the borehole containing fine grained granite. These intervals show also an increased natural gamma radiation. Granodiorite, diorite and gabbro show elevated density and susceptibility, where susceptibilities are high at certain locations due to high magnetite content. The seismic velocity of the rock is also increased where there is an occurrence of dioritic or gabbroic rocks.

Alteration in the rock is seen as an overprint on the different lithologies occurring in the area. Resistivity and acoustic velocity are typically decreased in altered sections. At the end of the borehole, the susceptibility log indicates low susceptibility level compared to elevated density which is indicating dioritic-gabbroic rocks. High ferrimagnetic magnetization typical to magnetite seems to be turned lower paramagnetic, likely due to hematitization.

Increased fracturing and some potentially hydraulically conductive fractures can be seen as a decrease in the resistivity or sonic velocity values, respectively. Sharp individual resistivity and velocity anomalies indicating possible significant fractures are seen as marked decrease in resistivity and acoustic velocity (sonic). These single fractures act also as sources generating tubewaves in the acoustic (Fullwave Sonic (FWS)) logging. Individual fractures are also seen in acoustic televiewer images and in the reprocessed computed caliper. Single fractures are also indicated by small changes in the borehole fluid temperature and in the electrical resistivity of borehole water.

Generally, the logging tools and the logging procedures functioned very well. The upward inclined borehole required special arrangements for filling up formation water into the borehole and for removal of air from the borehole. A customized sealing device with valves and water tight inlets for the logging cable and the air hose were designed for the logging exercise. Some unexpected malfunctions of the logging tools occurred. Natural gamma radiation logging was not carried out with a separate tool due to the break-down of the tool. The natural gamma values from the density tool were used, instead of production log data with natural gamma tool, as well as the optical televiewer’s internal (centralised) gamma values were used for length calibration of the density and natural gamma tools.

The normal resistivity and dual lateral log (DLL) values were found to be affected by the metallic connector of the air removal hose, resulting in decreased resistivity. This connector is not necessary to use in downwards inclined boreholes, but it was necessary to use this connector for upwards inclined boreholes like this one. The construction material for the connector was recommended to be non-conductive plastic, but a misunderstanding led to that the connector was constructed of brass

(non-magnetic). A replacement of the connector was not possible to perform during the field work. Initially it was considered impossible to make resistivity logging in a dry borehole. Dual laterolog operability was tested in a dry borehole. As the functionality was found reasonable, although not perfect in terms of resolution and noise, the borehole was re-measured in a dry state with a bridle electrode taking care of the grounding. This survey provided reasonably accurate and high resolution resistivity data from the borehole with dual laterolog (DLL shallow) data. The dual laterolog (DLL)-deep data are spurious and of low resolution. Normal logging was not repeated in the dry hole. Measured normal resistivities are very low because of the mentioned metallic objects near the probe.

Mechanical caliper logging was replaced with higher resolution caliper values and images computed from acoustic televiewer (ABI) travel time data. The computed ABI caliper results (diameter) show sudden, though minor level changes due to release of pressure in the borehole. This happened twice due to accidental release of a water hose connector (due to excess pressure). Because the caliper reading (diameter) is strongly dependent on borehole fluid acoustic velocity (due to salinity), temperature and pressure, and while it is experimentally fitted to the level of nominal borehole diameter, this incident caused a c. 0.5 mm jump in the diameter value which slowly returned to normal values as a function of increasing pressure. During the release of pressure in the borehole gas bubbles were emerging from the water, being clearly visible in amplitude on the upper side of the borehole image.

To avoid further damage to the valves and the air removal hose, the groundwater pressure was controlled after c. 60 m using intentional pressure releases using the valve. The depth and time of these pressure releases was not recorded. At these locations, at 3–5 m interval, the caliper reading (diameter) was smoothly increasing about 0.3 mm, then slowly decreased again as the pressure increased. According to the pressure gauge readings the pressure varied about 0–5 bar during the logging. These incidences were detected and checked during the logging operation, so their occurrence and cause was confirmed.

The KBS-3H design has been developed jointly by SKB and Posiva since 2002. This report has been prepared within the project phase “KBS-3H – System Design 2011–2016”.

Sammanfattning

Geofysisk borrhålsloggning genomfördes i borrhål K08028F01 i augusti 2014. Det genomförda arbetet utgjorde en fortsättning på den metodutveckling som påbörjats med mätningar i borrhål K03009F01 i februari 2014. I det aktuella arbetet genomfördes geofysisk borrhålsloggning för första gången i ett svagt uppåt lutat borrhål, som därmed krävde att borrhålet fylldes med vatten. Loggningsprogrammet inkluderade följande metoder; borrhålsvätskans temperatur och elektrisk konduktivitet, resistivitet (normal) och single point resistance (SPR), inducerad polarisation (IP), fokuserad resistivitet, fullvågssonic, densitet (gamma-gamma), naturlig gammastrålning, magnetisk susceptibilitet, och akustisk televiewer inklusive caliper.

Bergartskontakter, sprickor och flödande saltvatten kunde identifieras genom en första översiktlig granskning av insamlade data. Information om bergarter, omvandling och sprickighet från Boremap-karteringen användes för att längdjustera data insamlade i den aktuella loggningskampanjen. Rådata från loggningen omräknades till fysikaliska parametrar med hjälp av experimentella samband. Förhållanden kopplade till densitet (gamma-gamma) och magnetisk susceptibilitet justerades med utnyttjande av petrofysiska mätningar på bergprover från det aktuella borrhålet. Erhållna värden på resistivitet och p-vågshastighet jämfördes med petrofysiska mätresultat.

Resultat från den genomförda borrhålsloggningen indikerade geofysiska egenskaper och variabilitet längs borrhålet, indikerande förändringar i bergartsfördelning, sprickighet och förekomst av mer betydande sprickor (inklusive möjliga ”stora sprickor”). Densitet (gamma-gamma), naturlig gamma och susceptibilitet, och i viss mån gånghastighet från sonic bildar underlag för att beskriva variationen i bergartsfördelning. De huvudsakliga bergarterna uppvisar skilda densitetsvärden. Susceptibiliteten är generellt hög på grund av förhöjt innehåll av magnetit. Densitet och susceptibilitet är som lägst i de borrhålsintervall som innehåller finkornig granit. De senare intervallen karakteriseras även av en förhöjd naturlig gammastrålning. Granodiorit, diorit och gabbro visar förhöjd densitet och susceptibilitet, där susceptibiliteten är hög på vissa ställen på grund av förhöjt magnetitinnehåll. Bergets seismiska gånghastighet är också förhöjd där det finns förekomster bergarter med innehåll av diorit och gabbro.

Omvandling av berget kan ses som en överlagrad effekt på de olika bergartstyperna som förekommer i området. Resistivitet och akustisk gånghastighet kännetecknas typiskt av lägre värden i sektioner som karakteriseras av omvandling. Mot slutet av borrhålet indikerar susceptibilitetsloggen låga värden jämfört med en förhöjd densitet, som indikerar bergarter av dioritisk eller av gabbro karaktär. Hög ferromagnetisk magnetisering, typisk för magnetit, förefaller ha förskjutits mot en lägre magnetisering av paramagnetisk natur, förmodligen orsakad av hämatitisering.

Förhöjd sprickighet och några potentiellt vattenförande konduktiva sprickor kan skönjas i termer av reducerad resistivitet respektive lägre akustisk gånghastighet (sonic). Väldefinierade anomalier i resistivitet och gånghastighet indikerar möjliga signifikanta sprickor, i form av lokala minima i resistivitet och akustisk gånghastighet (sonic). Dessa enskilda sprickor fungerar även som källor för tubvågor som registreras och framträder i den akustiska fullvågssonic (FWS) loggningen. Individuella sprickor kan också identifieras i resultatbilder från akustisk televiewer och processerad caliper. Enskilda sprickor indikeras även av små förändringar i borrhålsvätskans temperatur och i dess elektriska ledningsförmåga.

Använd loggningsutrustning och tillämpade loggningsprocedurer har överlag fungerat väl. Det uppåtriktade borrhålet krävde speciella lösningar för att fylla upp hålet med formationsvatten, liksom för att evakuera luft från borrhålet. En specialutformad avtätningsutrustning med ventiler och vattentäta slussar för loggningskabel och luftslang konstruerades för den aktuella loggningen. Några oväntade felaktiga funktioner noterades hos loggningsutrustningen. Loggning med naturlig gamma genomfördes inte med en separat sond då den senare gick sönder. Istället användes värden på naturlig gamma från densitetssonden för att generera produktionsdata, där även värden från optisk televiewer (intern centraliserad gamma) användes för längdkalibrering av sonder för densitet och naturlig gamma.

Det noterades att värden från resistivitetsloggarna (normal och dual laterolog (DLL)) var påverkade av metallkopplingen för luftslangen, vilket resulterande i reducerad resistivitet. Denna koppling behövs inte i nedåtriktade borrhål, men är nödvändig i uppåtriktade borrhål, som i det aktuella fallet. Användning av icke ledande plast hade rekommenderats som konstruktionsmaterial för kopplingen, men ett missförstånd ledde till att kopplingen tillverkades av mässing (icke magnetisk). Utbyte av kopplingen var inte möjlig att utföra i samband med arbetet i fält. Inledningsvis betraktades det som omöjligt att genomföra resistivitetsloggning i ett torrt borrhål. Ett test med dual laterolog (DLL) utfördes i torrt hål. Då acceptabel funktionalitet uppnåddes, om än inte helt perfekt vad avser upplösning och brus, mättes borrhålet på nytt med en s k bridle-elektrod som möjliggjorde jordning. Denna undersökning gav någorlunda exakta och högupplösta resistivitetsvärden med dual laterolog (DLL)- shallow. Data från dual laterolog (DLL)-deep uppvisar mer diskutabla och lågupplösta resultat jämfört med resultaten från dual laterolog (DLL)- shallow. Resistivitetsloggning (normal) upprepades inte i torrt hål. Mätta resistiviteter (normal) är mycket låga på grund av tidigare nämnt metalliskt objekt nära sonden.

Mekanisk caliperloggning ersattes med calipervärden beräknade från gångtidsdata från Akustisk Televiewer (ABI) och tillhörande bilder. Beräknade caliperdata (diameter) från ABI uppvisar plötsliga, om än mindre, förändringar i nivå orsakade av tryckavlastningar i borrhålet. Detta hände två gånger på grund av oavsiktlig lossning av kopplingen till vattenslangen (på grund av för högt tryck). Då caliperbestämningen (diameter) är starkt beroende av ljudhastigheten i borrhålsvätskan (beroende på salthalt), temperatur och grundvattentryck, och beroende på experimentell anpassning till nominell borrhålsdiameter, innebar denna händelse en ca 0,5 mm hopp i diametervärdet, som sakta återhämtade sig till normala nivåer som funktion av ökat vattentryck. Vid sänkning av grundvattentrycket i borrhålet frigjordes också gasbubblor i vattnet, tydligt märkbara i amplituden i bilderna på ovansidan av borrhålet (upp).

För att undvika skador på ventiler och slang för evakuering av luft, kontrollerades grundvatten-trycket efter ca 60 m med hjälp av medvetna trycksänkningar. Djupet och tidpunkten för dessa tryck-sänkningar noterades dock inte. På dessa djup, över intervall på 3–5 m, ökade caliper-värdena (diameter) gradvis med ca 0,3 mm, och minskade sedan åter gradvis när grundvattentrycket ökade. Enligt tryckgivarna varierade trycket mellan 0–5 bar under loggningen. Dessa händelser identifierades och kontrollerades under loggningsförloppet, verifierande att de ägt rum och möjlig orsak till dessa.

KBS-3H är en variant av KBS-3 metoden som utvecklats gemensamt av SKB och Posiva sedan 2002. Denna rapport har utarbetats under projektfasen ”KBS-3H – System Design 2011–2016”.

Contents

1 Introduction 9

2 Objective and scope 11

3 Equipment and survey procedure 13
3.1 Equipment 13
3.2 Sealing device 13
3.3 Description of logging equipment 16
3.4 Description of surveys 17
3.4.1 Fluid temperature and conductivity surveys 17
3.4.2 Normal resistivity, single point resistance and induced polarization surveys 17
3.4.3 Focused resistivity 18
3.4.4 Full waveform sonic 18
3.4.5 Density and natural gamma radiation surveys 19
3.4.6 Magnetic susceptibility 19
3.4.7 Caliper survey 19
3.4.8 Acoustic imaging 19

4 Performance 21
4.1 General 21
4.2 Calibration measurements 21
4.3 Execution of field work 21
4.4 Data handling and post-processing 23
4.4.1 Length adjustments 23
4.4.2 Post-processing using petrophysical data 23
4.4.3 Post-processing of other logging data 25
4.5 Analyses and interpretations 27
4.6 Nonconformities 28

5 Results and discussion 31

6 Concluding remarks 37

References 39

Appendix 1 Review of appendices 41
Appendix 2 Field activity time log 45
Appendix 3 Petrophysical data from samples 49
Appendix 4 Geophysical Properties 51
Appendix 5 Fluid Properties 53
Appendix 6 Acoustic Hole Imaging 55
Appendix 7 Rock Mechanical Properties 65
Appendix 8 Full Waveform Sonic 67
Appendix 9 Full Waveform Sonic, wideband log 69
Appendix 10 Full Waveform Sonic, chevron plot 71
Appendix 11 Full Waveform Sonic, tubewave plot 73

1 Introduction

This document reports the field operations and data collected by the geophysical logging of borehole K08028F01 in the Äspö Hard Rock Laboratory (Äspö HRL). Borehole K08028F01 was core drilled in the Äspö Hard Rock Laboratory in 2014 as partof the KBS-3H Sub-Project Sub System Demonstration, 2011–2016 , in part. The work is in part linked to a task to reassess the borehole geophysical logging methods and measurement settings in boreholes drilled from tunnels, for example to characterize significant fractures and deformation zones in the bedrock. This work is a continuation of the earlier measurement campaign of borehole K03009F01 drilled in the same rock volume in Äspö HRL. The latter borehole was slightly downward inclined whereas the one being the focus of the current work is slightly upward inclined. The logging methods and settings were tested and analyzed in the previous work, and the reassessed and decided settings were adopted in the application for the current borehole, i.e. K08028F01.

In Table 1-1 the controlling documents for performing this activity are listed.

Table 1-1. Controlling documents for the performance of the activity. All documents are SKB unpublished internal documents.

Activity plan	Number	Version
Name	AP TD 3HDEMO-14-045	1.0
Method descriptions	Number	Version
Name	SKB MD 221.002	3.0

Geophysical borehole logging of borehole K08028F01 (Table 1-2, and Figure 1-1 and Figure 1-2) at Äspö Hard Rock Laboratory was carried out 25th–29th of August 2014. The assignment included the following logs: fluid temperature and electrical conductivity, normal resistivity and single point resistivity (SPR), induced polarization (IP), focused resistivity, full waveform sonic, gamma-gamma density, natural gamma radiation, magnetic susceptibility, caliper and acoustic imaging.

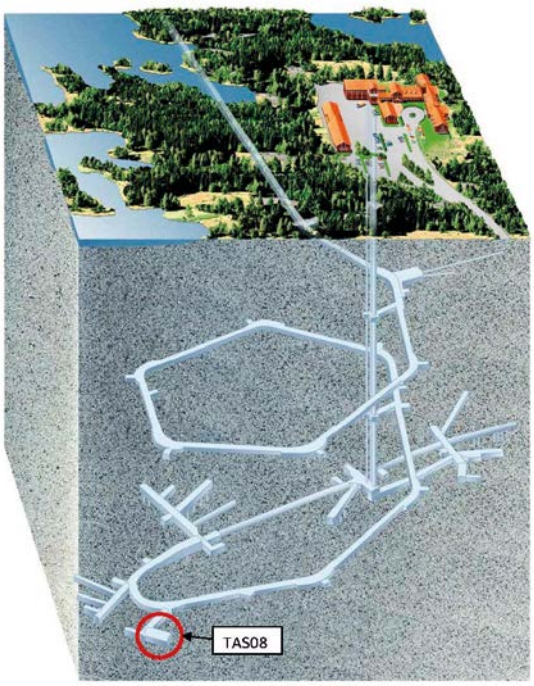

Figure 1-1. *Overview of the location of tunnel TAS08, which is the location of the borehole K08028F01 at Äspö laboratory on level −400 m.*

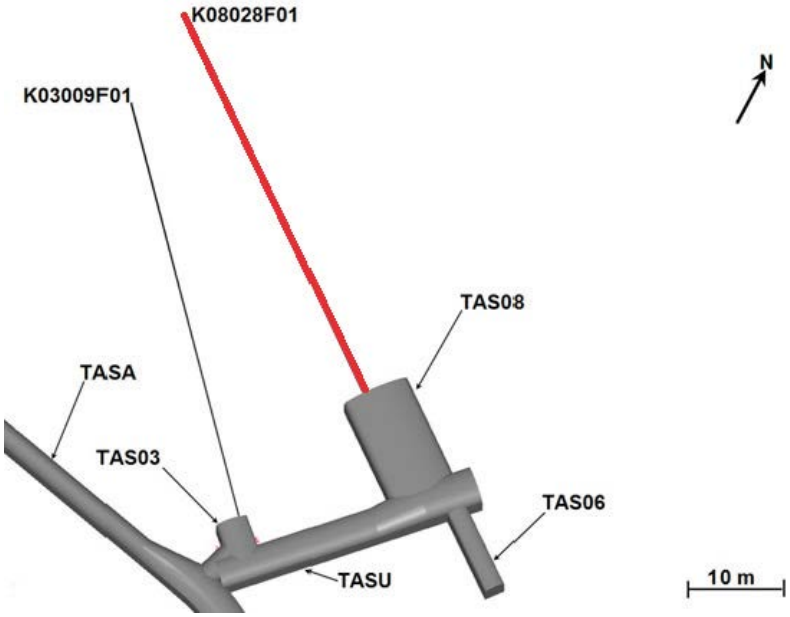

Figure 1-2. *Location of borehole K08028F01 in tunnel TAS08. Borehole K03009F01 in the neighbouring tunnel TAS03 is indicated for reference.*

Table 1-2. Technical data of borehole K08028F01.

Borehole **Site**	**K08028F01 (rock surface)** **Äspö Hard Rock Laboratory, TAS08**			
Coordinate system	RT90/RHB70		ÄSPÖ96	
Coordinates for starting point	Northing Easting Elevation	6368,033.714 1551,637.131 −396.584	Northing Easting Elevation	7,450.637 2,368.035 −396.584
Direction (°)	308.5431		320.370	
Inclination (°)	2.18		2.18	
Drilling diameter (mm)	75.8		75.8	
Length (m)	94.39		94.39	
TOC-reference level (m)	0.347		0.347	

The field work was coordinated by geophysicist Karla Tiensuu and geophysical foreman Antero Saukko. The field survey team consisted of Antero Saukko and Henri Luiro. Quality control of raw data, data processing and integration as well as interpretation of sonic data was conducted by geophysicist Eero Heikkinen of Pöyry Finland Oy. Reporting was conducted by geophysicist Karla Tiensuu and Eero Heikkinen.

The original survey results as well as necessary calibration files have been delivered to SKB for storage in the SICADA data base. Files can be found given their association with the activity plan number AP TD 3HDEMO-14-045.

The KBS-3H design has been developed jointly by SKB and Posiva since 2002. This report has been prepared within the project phase “KBS-3H – System Design 2011–2016”.

2 Objective and scope

The borehole geophysics contributes to detection of large fractures and deformation zones and their orientation and the description of the bedrock quality and properties at the survey site. The employed methods provide valuable assistance, in the context of a repository for spent nuclear fuel, for defining stable and homogeneous bedrock blocks for deposition. Also defined are large fractures that may constitute a potential risk for secondary movements in case of future seismic events.

3 Equipment and survey procedure

3.1 Equipment

The geophysical borehole logging program was performed in six logging runs and two repeat runs. The equipment is listed in Table 3-1.

Table 3-1. Used geophysical logging methods and equipment with their respective serial numbers.

Method	Equipment (with serial numbers)
Fluid temperature and fluid conductivity.	QL40 FTC Fluid Temperature and Conductivity Probe, S/N 5715.
Normal resistivity (8, 16, 32 and 64 inch), single point resistance, induced polarisation.	QL40 ELOG IP Probe, S/N 5782.
Focused resistivity.	GeoVista DLL3 Probe, S/N 124801.
Full waveform sonic.	QL40 FWS Probe, S/N 130607
Density (gamma-gamma).	GeoVista Slimhole Density Probe, S/N 4490.
Natural gamma radiation.	GeoVista Slimhole Density Probe, S/N 4490 (QL40 GRA Probe, S/N 5493 was broken).
Magnetic susceptibility.	QL40 MagSus Probe, (Bartington BSS-02B-2), S/N 103114, magnetic test block, S/N 047.
Acoustic imaging.	ABI 40 Probe, S/N 092801.
Acquisition system.	ALT Matrix, S/N 0612.
Acquisition system.	ALT Bbox, S/N 124311.

Fluid resistivity and temperature and sonic logging as well as acoustic imaging strictly require water filling in the borehole. Natural gamma, gamma-gamma density and susceptibility benefit from keeping the water in the borehole. Calibration will be different and varying depending on the water filling in the borehole. The resistivity measurements have weaker resolution in a dry borehole and show spurious results and significant noise in places, and it is estimated there should be at least a thin film of water in the borehole to allow acquisition of good data.

3.2 Sealing device

The applied working routines were quite straightforward. At all times when logging was not active, the valve at the borehole collar was kept closed and the borehole was allowed to be filled with water. Natural inflow was c. 1.5 litres per minute. Each logging run took some additional time due to the upward inclination of the borehole. The rod feeding rig was necessary to move the probe to starting position at the end of the borehole. Because all applied methods were requiring, or benefitted significantly from water filling of the borehole and removal of air from the borehole, the borehole was closed at the collar using a new borehole sealing mechanism, used for the first time during these measurements. The sealing mechanism was developed by Pöyry Finland Oy through a SKB-Posiva co-operation. The sealing device was designed by Jari Pöllänen (Pöyry) and constructed by Terra Team Oy (Finland) (Komulainen and Pöllänen 2016). Some minor changes for the geophysical surveys were designed by Antero Saukko (SMOY) and constructed by Terra-Team Oy.

The sealing device included a bushing (inlet) for the logging cable and its connector and for the air hose which was used to remove air from the end of the borehole. The sealing device was made of acid-proof steel and its internal parts were sealed with graphite-impregnated polyurethane seals. The sealing device is shown in Figure 3-1and Figure 3-2. A valve was used to feed in the water that

replaced the air. Both the logging cable and the air hose followed the probe when it was moved into the borehole using push rods, by way of the rod feeding rig. The probe was inserted by the rod rig to a one metre distance from the end of the borehole. The final metre was moved manually until the end of the borehole was felt by the push rods. The push rods were subsequently removed from the borehole.

After the probe was at its starting position, the sealing device was attached to the collar of the borehole and secured water tight. The water used to fill the borehole was Äspö formation water to ensure that there would be no changes introduced to the water chemical composition. The carbon dioxide and oxygen of the atmosphere were removed by allowing nitrogen gas into the 1 m^3 water tank at 5 bar pressure, over 1 hour time each day before startup. The pH of the water was measured twice during the week and found acceptable, being close to 7.

Finally the borehole was filled with water, and air was simultaneously removed from the end of the borehole. When the borehole was filled of water, the air hose was released from its connector using air pulse from a compressor, then the air hose was removed from the borehole by way of the inlet, and the bushing was closed before the logging started.

Figure 3-1. *The sealing device. The wide part is fastened onto the borehole bushing. The outermost part is fastened after removing the push rods and the air hose. The logging cable runs through the whole device.*

Figure 3-2. *The outermost part of the sealing device opened up on the work bench.*

The overall survey procedure was as follows:

1. In the beginning of each survey day the water in the tank was nitrogenated.
2. The borehole water valve was opened.
3. The borehole water was left to run back to the tank located at the collar, and the excess was disposed of to drain.
4. The cable head was directed through the sealing device. A survey probe was attached to the cable. The air hose and pushing rods were connected to the cable head, using a connecting piece.
5. The survey probe was pushed to the end of the hole using pushing rods with the rod feeding rig.
6. Pushing rods were pulled out of the borehole.
7. The components of the sealing device were assembled onto borehole collar (around the cable). The sealing device for the logging cable and the air hose was closed.
8. The borehole was filled with stored water using a pump, simultaneously allowing removal of air from the bottom of the borehole. The water volume in the borehole was approximately 430 litres.
9. The air hose was removed from the borehole and the bushing was closed.
10. The logging was done towards the collar of the borehole. Pressure was regulated manually to avoid leakage through the sealing device.
11. The sealing device was opened and the water was allowed to flow out of the borehole, back to the water tank.
12. The survey probe was changed and the procedure (starting from step 3) was repeated. Data quality was analyzed immediately on site to decide on possible need of repetition.
13. At the end of each survey day the borehole valve was closed and time of closure documented in the daily log.

3.3 Description of logging equipment

The geophysical survey carried out in K08028F01 borehole included fluid temperature and resistivity, normal resistivity (8”, 16”, 32” and 64” arrays) including single point resistivity (SPR) and induced polarization (IP), dual laterolog focused resistivity, full waveform sonic, gamma-gamma density, magnetic susceptibility and acoustic televiewer imaging.

The natural gamma radiation survey using a separate probe was included in the survey plan, but unfortunately the probe turned out broken. The natural gamma sensor (NaI crystal of 25×50 mm) integrated within the slimhole density tool was used instead. Caliper measurement was also included in the survey plan, but it was excluded as the caliper data obtained from the acoustic imaging data was considered sufficient.

The data acquisition system was ALT Matrix S/N 0612 for all surveys apart from the electrical logs. The electrical methods (normal resistivity, single point resistance, induced polarisation and focused resistivity) were operated with ALT BBox (S/N 124311), which enabled replacing the bridle connector for remote return current with a fixed electrode grounded outside the borehole.

Fluid temperature and conductivity were measured in the same run as the full waveform sonic. Fluid resistivity and sonic probes were connected to each other with quick link system (QL40). The fluid temperature and conductivity probe were closest to the end of the borehole. Full waveform sonic was later measured separately using only one channel with long 16 ms recording time, also.

A list of the survey methods, equipment used and the basic survey parameters is shown in Table 3-2.

Table 3-2. Used methods, equipment and survey parameters.

Method	Acqui-sition system	Equipment	Logging direction	Logging speed (m/min)	Point spacing (m)	Note
Fluid temperature and conductivity.	ALT Matrix	ALT QL40 FTC Fluid Temperature and Conductivity Probe.	Back	1	0.02	Centralised, run with FWS.
Full waveform sonic (four channels, 4 ms time range).	ALT Matrix	ALT QL40 FWS Probe.	Back	1	0.02	Centralised.
Full waveform sonic, 1 m transmitter-receiver channel, 16 ms time range.	ALT Matrix	ALT QL40 FWS Probe.	Back	1.3	0.05	Centralised.
Normal resistivity (8, 16, 32 and 64 inch), induced polarisation.	ALT BBOX	ALT QL40 ELOG IP Probe.	Back	3	0.02	Non centralised.
Focused resistivity (water filled and dry hole).	ALT BBOX ALT Matrix	GeoVista DLL3 Probe.	Back	3	0.02	Non centralised.
Density (gamma-gamma) and natural gamma radiation.	ALT Matrix	GeoVista Slimhole Density Probe.	Back	2	0.02	Non centralised.
Magnetic susceptibility.	ALT Matrix	ALT QL40 MagSus Probe.	Back	2	0.02	Non centralised.
Acoustic imaging.	ALT Matrix	ALT ABI 40 Probe.	Back	0.53	0.0015	Centralised.

The various logging tools were pushed into the borehole with pushing rods or pushed with an electrically powered rod feeding rig because of the slightly upward inclined borehole. The rod feeding rig was used for insertion of the equipment, while during the measurement run, moving the probe and triggering of data storage was done with the cable, when logging outwards.

Surveys were done from the end of the borehole towards the collar with varying settings for data storage and logging rate. Depth range of recorded data varied according to method and it is dependent on the position where each sensor (the reading point) is located in the probe. Stacked or integrated probes limit the depth range further, leading to some of the data sets (profiles) to start at 1–1.5 m from end of the borehole. The outer part of the borehole was measured entirely to the collar. The results were delivered and plotted covering the actual measurement range.

The cable was operated by an electrically powered winch. Depth measurement was triggered by pulses of a sensitive depth encoder, installed on a pulley wheel. A 280 m long, 3/16" steel reinforced 4-conductor cable manufactured by Mount Sopris was used in the logging. The cable came with 10 m markers enabling control of depth measurement and for facilitating adjustment for any occurring cable slip or stretch.

Stackable QL40 tools were connected to the cable head with tool top QL40-G04. Special plastic centralisers were used for the acoustic imaging and full waveform sonic logging.

3.4 Description of surveys

3.4.1 Fluid temperature and conductivity surveys

Fluid temperature and conductivity logs were conducted with ALT QL40 FTC Fluid temperature and Conductivity Probe. The QL40 FTC provides borehole temperature and fluid conductivity measurements over a wide range of conductivity from fresh to saline water. The tool is designed in such a way that the optimal survey direction is downwards (into the borehole). Normally the measurement procedure in Äspö has included stabilization of borehole water over several days before fluid temperature and conductivity logging. The backward logging direction from the end of the borehole, and filling of the borehole (though with locally extracted water) immediately before the startup of logging run, will certainly affect the representativity of the results. What is expected to be obtained from the logging, are local changes in temperature and conductivity profiles due to inflow or outflow of water at fracture locations.

Fluid electrical conductivity and temperature were measured simultaneously with full waveform sonic measurement, probes were stacked together with Quick Link –adapter.

Fluid temperature is measured with a sensor based on a fast response semiconductor device whose output voltage varies linearly with temperature. The temperature sensor is located in a stinger at the top of the sensor body at the centre of the three exit ports where the borehole fluid returns to the borehole. Fluid conductivity is measured using a seven electrode mirrored Wenner array, assembled inside a cylinder at the end of the probe. The cylinder is open towards the end of the probe and has small holes above the conductivity sensor, allowing the water to flow through the sensor.

Borehole water passes by the array as the probe is introduced into the borehole. The array is completely shielded from the borehole wall, such that only the fluid conductivity, and not borehole wall conductivity, is measured. The tool has a diameter of 43 mm and a length of 0.78 m. Recording point is 0.1 m from the end of the borehole.

The tool is calibrated by the manufacturer. However, an independent calibration was carried out by SMOY as part this survey program. Calibrations are discussed in more detail in Section 4.2.

3.4.2 Normal resistivity, single point resistance and induced polarization surveys

Normal resistivity, single point resistance and induced polarization were surveyed with the Mount Sopris QL40 ELOG Probe. The QL40 ELOG provides four normal resistivity measurements (N8", N16", N32" and N64"), as well as spontaneous potential (SP) and single point resistance. In addition, the IP function provides two digital induced polarization (IP) channels.

The IP uses the 16“and 64” separation between voltage and current electrodes. The probe measures the injection and relaxation voltages on both measurement electrodes as a function of time. This measurement is digitized and presented as 10 channels of time based data per depth interval for each electrode spacing. In addition, a high resolution A/D converter further divides each channel into 10 more discrete samples, providing a “full wave” presentation of the injection and relaxation decay. The data are then transmitted in the wireline using a pulse coded digital data protocol. A charge-ability value (“ma”) is integrated for both N16” and N64” from the IP windows.

The measurement range of the normal resistivity measurement is from 0.1 Ωm to 100 000 Ωm. The tool has a diameter of 43 mm and a length of 1.90 m. Single point resistance electrode (and current electrode) distance from the end of the probe is 0.06 m. The 8” potential electrode is 0.26 m, 16” 0.47 m, 32” 0.87m and 64” 1.68 m from the end of the probe. The recording points projected to the middle of interval were 0.06 m for SPR, 0.16 m for 8”, 0.26 m for 16”, 0.47 for 32” and 0.87 m for 64” interval from the end of the probe.

Return current is arranged either on an isolator bridle where current electrode is 12.4 m above the active electrode array or by placing a reference electrode outside the borehole, which was the case in this survey.

Calibrations are discussed in Section 4.2.

3.4.3 Focused resistivity

Focused resistivity measurements were carried out using Geovista’s Dual Laterolog-3 (DLL3) resistivity probe. Focused laterolog resistivity tool measures bulk resistivity of the bedrock by injecting the current through multiple current electrodes set at the same electrical potential, and placed at several distances above and below the dipole voltage measurement array. Compensated voltage is measured using a closely spaced dipole in the middle of the array. The electrode construction and configuration of the tool is designed so that electric current is injected onto a planar disk perpendicular to the borehole, centered on the voltage dipole.

Following measurement of current and potential, their ratio is computed and presented as two resistivity values that correspond to different penetration of current out from the borehole. The electrode geometry of the tool enables good compensation of borehole groundwater electrical conductivity variation, and provides good sensitivity and location accuracy for detected fractures. Performance is generally better than the one obtained with normal resistivity probe.

Return current is arranged either on an isolator bridle which is 10 m separated from the active electrode array or by placing a reference electrode outside the borehole. In this survey both types of grounding method were employed, while the pushing rod connector was unfortunately made of brass, and therefore affected the results when logging with reference electrode outside the borehole. Metal push rods were extended with glass fibre push rods for the 10 metres closest to the probe to avoid interference with electrically conductive borehole water.

Surveying with a bridle was only done in a dry borehole. These results were rather good for DLL3 Shallow resistivity, so the borehole walls were probably wet enough to ensure sufficient connection. The DLL3 Deep was suffering from a low current level and exhibits very high and partly spurious values.

The tool has a diameter of 42 mm and a length of 2.37 m. The observation point is 1.18 m from the end of the probe. For the ALT DLL-3 tool used with BBox the distance of the observation point from the end of the probe is 1.25 m and the length of the probe 3.01 m.

Calibrations are discussed in Section 4.2.

3.4.4 Full waveform sonic

Full waveform sonic measurements were conducted with the Advanced Logic Technology’s (ALT) QL40 FWS equipment. A piezoceramic transmitter (Tx) emits sonic pulses of 6 kHz nominal frequency with four receivers (Rx1, Rx2, Rx3 and Rx4) detecting the arriving impulses. The arriving

waveform is digitally sampled according to the tool configuration parameters. The Tx to Rx spacings are 0.6 m (Rx1), 0.8 m (Rx2), 1.0 m (Rx3) and 1.2 m (Rx4), respectively. The diameter of the tool is 50 mm. The tool was connected with FTC fluid temperature and conductivity probe which was located as a bottom extension enabling proper centralizing. The tool was centralized with non-flexible plastic centralizers on top and bottom. The combined length of the sonic and fluid resistivity probe was 3.04 m. Sonic receiver Rx1 was 0.96 m from the end of the probe, transmitter at 0.36 m, and the recording point projected to the middle of the transmitter were for Rx1 – Tx at 0.66 m, Rx2 – Tx at 0.76 m, Rx3 – Tx at 0.86 m and for Rx4 – Tx at 0.96 m.

3.4.5 Density and natural gamma radiation surveys

Gamma-gamma density and natural gamma radiation were measured with an integrated GeoVista slimhole density probe. Survey data from both parameters were obtained from the same depths in one single run. The probe uses a 10 mCi cesium source (^{137}Cs). The probe measures simultaneously the natural gamma radiation over 134 cm and two gamma-gamma counts over different distances from the source (SSD, 11 cm and LSD, 22 cm). The detectors are 50 × 25 mm NaI crystals. Recording time is 0.22 seconds. The density probe has a diameter of 38 mm and a length of 1.65 m. The SSD density recording point is at 0.16 cm from the end of the probe, LSD is 0.28 m from the end. The natural gamma recording point is 1.39 m from the end of the probe. The separate ALT QL GRA probe was broken, so the planned more accurate natural gamma survey was replaced by the sensor that integrated with the density probe. For the same reason the planned natural gamma depth reference between most of the borehole runs was not possible.

3.4.6 Magnetic susceptibility

Magnetic susceptibility was measured using a QL40 MagSus magnetic susceptibility probe (Bartington sensor). The probe has two parts: the focused dual coil detector is located in a non-magnetic enclosure and the electronics is hosted in an aluminum alloy cylindrical enclosure. The probe uses an operating frequency of 1.5 kHz. Electromagnetic coil separation is designed such that a magnetized zone with minimum thickness of 0.12 m is detected with its real dimensions, whereas narrower zone thicknesses are exaggerated.

The susceptibility probe has a diameter of 43 mm and a length of 1.4 m. The recording point of the probe is 0.19 m from the end of the probe.

Calibration measurements for the magnetic susceptibility probe were run both before and after the borehole survey. Calibrations are discussed in more detail in Section 4.2.

3.4.7 Caliper survey

The borehole caliper measurement was included in the survey plan, but was excluded as caliper computed from the acoustic imaging was considered sufficient, based on previous experience.

3.4.8 Acoustic imaging

Acoustic imaging was carried out using Advanced Logic Technology's (ALT) ABI40 acoustic borehole televiewer. The ABI40 probe creates a 360 degree image of the borehole wall by using acoustic ultrasound pulses (1.2 MHz) and recording the amplitude and travel time of the returning signal. Measurement of borehole orientation in 3D space is controlled with a 3-axis magnetometer and three accelerometers, respectively. Thus, it is possible to measure borehole deviation data and create accurate orientation of the acoustic images.

The sampling rate is 72, 144 or 288 measured points per revolution depending on operator selection. The width of acoustic beam is 1.5 mm. Both longitudinal and azimuthal resolution is restricted by the width of the acoustic beam, i.e. 1.5 mm, although also smaller features can be detected although their thickness is exaggerated. The detection limit for geological structures (in terms of thickness) is in the order of tens of micrometers. The survey rate is 0.5–1 m/min. The ABI40 tool diameter is 40 mm, but due to need of focusing the acoustic beam, a borehole diameter less than 51 mm (2 inches) cannot be measured.

In order to obtain good quality data, proper centralizing of the tool is of utmost importance. In near-horizontal boreholes especially, non-flexible centralizers are required. Data quality is also sensitive to the logging direction. Downward (in to the borehole) logging is the primary option, which is to be used if it is possible to achieve a smooth movement of the probe. Every abrupt change in movement will entail loss of data (points). Proper functioning of the probe in nearly horizontal boreholes apparently requires sufficient groundwater pressure, which was attained using the borehole sealing device.

The tool diameter is 40 mm with a length of 1.6 m. The recording point of the probe is 0.16 m from the end of the probe.

4 Performance

4.1 General

For all of the methods, the logging direction was from the end of the borehole towards the collar. This was due to the requirement for filling the borehole with water, installation of the probe to end of the borehole using push rods/rod feeding rig, and sealing of the borehole. Outward movement was enabled by a motorized winch and 4-conductor armoured wireline, which also provided data transfer and communications connection to the probe. The probe length position in the borehole was stored using pulley wheel equipped with a sensitive depth/length encoder. Cable marker locations were stored in excel file together with encoder readings.

4.2 Calibration measurements

Calibration measurements were done for the ELOG resistivity and IP, DLL resistivity and susceptibility probes during the field work, and the results were stored. Calibration resistor boxes or known magnetized substances provided by manufacturers were applied for the probes to record data in time mode. Density and fluid resistivity and temperature probes were using previously defined calibrations. Natural gamma and full wave sonic, as well as acoustic televiewer probes do not require calibration. Susceptibility and gamma-gamma density raw data were further converted to physical values using petrophysical data obtained from the same borehole.

The rented QL40 ELOG + IP probe S/N 5782 for normal resistivity, single point resistance and induced polarization were calibrated on August 26th, 2014 prior to the actual ELOG measurements. The ELOG calibrator resistor box was connected to the probe, and different resistance values were switched on while recording data file in time mode.

The rented focused resistivity probe (Geovista DLL3 S/N 124801) was calibrated by recording data with the DLL3 calibrating resistor box connected to the probe. The calibration was done on August 26th, 2014 and the actual in situ survey was done the following day. Calibration files were stored accordingly.

The magnetic susceptibility probe (BSS-02B-2 S/N 103114) was calibrated both immediately before and after the borehole logging run. Calibrations were made on August 28th, 2014, when the probe had been on site for two days, so that its internal temperature had adjusted to ambient conditions. Calibration measurements were done with different materials: in air and with a calibration ring having a susceptibility value of $199*10^{-5}$ cgs, both with and without keeping a hand on the probe. Keeping a hand on probe lowers the values with 16 units and simulates the effect of contact with groundwater. Calibration data were stored for later use.

4.3 Execution of field work

Each technique used is briefly described below in connection to the results presentation. For detailed descriptions, the reader is referred to the method descriptions.

Work started on August 25th with site introduction, mobilization on the borehole in the tunnel and an introduction of the rod feeding rig functions. Probes were allowed to stabilize for temperature in the working area.

The water in the water tank was bubbled with nitrogen gas first thing each working day. Nitrogenation of the water was ongoing during survey preparations. Subsequently, the water valve was opened and the borehole fluid was allowed to flow out of the borehole, primarily to the tank, and excess water was led to an installed drain.

Each logging run was initialised by mounting the parts of the QL40 tools together when applicable, assembly of centralisers if required, attachment of the cable head to the probe, and placement of the tool onto borehole collar. Tool dimensions from bottom to top and the recording point of the tool from the cable connector and from the end of the tool were measured and used in defining the borehole length and location of the recording point when starting the pushing of the probe towards the end of the borehole, and starting the logging from the end of the borehole. Cable markers at 10 m interval were read from a constant place (cable guide) and this length was written in Excel file during logging run. The distance of the cable marker reading point both from the cable connector and from the recording point were also written into the Excel file. These were used when checking the length position and for making necessary corrections.

Probe, encoder wheel and winch were connected to either the ALT Matrix logger unit or the ALT BBox logger unit. The logger unit was connected to a field computer using an USB connector.

During startup, measurement parameters and telemetric settings for each probe were set in the logging software. Stackable tool dimensions were set.

The probe was attached to the cable, the air hose and pushing rods. Initially the probe cable connector was placed at the collar top, and the recording point in the probe depth was calculated using the measured distance from the cable connector to the recording point. Probe depth was set to this value as a starting position for the inward motion. This would mean that the zero reading in the file corresponds to a situation where the recording point is exactly at the rock surface.

Then the probe was pushed with the rods using the rod feeding rig to the end of the borehole. As the probe reached the end of the borehole or other defined borehole length, the rods were removed from the borehole.

Probe depth value (starting depth) at the end of the borehole was set in the logging software to a reading where the actual observation point was located. This measurement point position from the end of the borehole was computed using the measured length between end of the probe and the recording point, and also the known end of the borehole. This was known since the tool had been pushed carefully against end of the borehole, and a precise reading point of the sensor (for example 16 cm backwards from end of the borehole for density probe) was measured from the probe. The length of a given reading point from the end of the borehole was subtracted from the borehole length to obtain this value.

Measurement direction and data sampling length rate were set. Typical sample rate was 1/0.02 m except for acoustic televiewer, for which it was 1/0.0015 m.

The sealing device for the cable and the air hose was closed. The borehole was filled with water using a pump, allowing water to displace the air in the borehole after which the air hose was removed.

After removing the air hose the logging was started. Associated data file was initialized. Settings were stored in data file.

During the logging, the probe was pulled with the cable from the end of the borehole towards the collar. Data storage was launched by pulses sent from the encoder wheel at borehole collar. Performance of logging and the measurement results were reviewed throughout the run, for example by minimising signal error levels (missing data) by tuning of logging speed rate. Cable length marker locations for cable and logger unit readings were stored in an Excel file at a 10 m interval.

After each survey the sealing device was opened and water was allowed to run out of the borehole, back into the water tank. After that the survey probe was changed to the next one and the procedure was repeated. At the end of each survey day the borehole valve was closed.

Each logging was recorded in a new data file. Data was checked immediately for quality control, and a new logging run was initialised.

Times for different tasks were recorded in survey protocols. Filled-in forms were delivered to SKB after completion of the field work.

Survey activities are listed in Appendix 2.

4.4 Data handling and post-processing

At the end of each logging run the resulting data file was stored on a computer. Data files were opened with WellCAD software and results checked for quality and decision on whether possible repeated measurements were to be made.

Descriptions of raw data were prepared together with an associated data file structure. Logging profile raw data were stored in WellCAD 4.2 format and logging ASCII format (*LAS). The data file structure was handed over to SKB's representative at the end of the field work.

4.4.1 Length adjustments

Post-processing consisted of length adjustments and computation of physical parameter values from the acquired raw data. For sections subject to repeated logging, the data set deemed being of highest quality was used in the subsequent processing (Normal Resistivity and Dual Laterolog).

Length matching was carried out by collecting information on length differences between drillcore (true) and logging (recorded) data. The core geological data (lithology and fractures) from Boremap were available for length management. Also the previously measured OBI50 optical televiewer data including natural gamma was made available and used for length matching.

The end of casing when visible in the data, the end of borehole with respect to deepest obtainable data value (measurement point of tool above the end of borehole) and the cable marker differences to recorded length were calculated. Borehole end was felt physically when pushing the probe manually to the bottom. Geological marker points detectable from each logging method were collected and differences to recorded length were calculated.

For length adjustment of each data set, differences between measured borehole length value, and geologically defined true position were computed. A piecewise linear function was fitted on these observations, and imported to WellCAD software as a new Depth Log.

Using this created Depth Log, the borehole length values were recalculated in WellCAD to correspond the true probe positions in the final data files.

Length corrections by each method were based on the rules defined in Table 4-1.

4.4.2 Post-processing using petrophysical data

Recorded raw data values were converted to physical values with experimental ratios. Counts per second values of gamma-gamma density and natural gamma radiation were computed to bulk density (kg/m^3) and exposure values (µR/h). Susceptibility was converted from recorded voltage values to susceptibility (10^{-5} SI). Resistivity records were converted from Ohm values (ratio of voltage and current) to resistivity values using geometric factors and calibration ratios.

Calibrations were applying tool-specific calibrators for susceptibility (block of known susceptibility and air) and resistivity (known resistors). Further to calibrator values, the gamma-gamma density and susceptibility applied for re-calibration the petrophysical data from samples taken from the core obtained from the borehole.

Samples were selected after borehole logging by Oskar Sigurdsson and Eero Heikkinen. Selection was based on representative location from several lithological units, from intervals displaying fairly even levels of different geophysical data sets. Each sample was selected so that there were no intersecting fractures. Lithology and deformation were described. Samples were cut by Pierre Nilsson with a saw to length of 50 mm. Surfaces were cut even.

Samples were analyzed for petrophysical values of density, susceptibility, remanent magnetization, seismic P-wave velocity, electrical resistivity and porosity by the Geological Survey of Finland, Espoo. Porosity was defined by weighing the samples dry and saturated. Saturation took several weeks in tap water. Drying of samples required three days in an electric oven at 90 °C. Seismic P-wave velocity and resistivity were measured on saturated samples. Seismic velocity was measured at un-loaded conditions. Resistivity was measured with three frequencies (0.1, 10 and 500 Hz). Induced polarization frequency effect (%) was computed from the resistivities at different frequencies. Results from the analysis are listed in Appendix 3.

Table 4-1. Order and general principles of performed length adjustments.

Logging method	Length references visible in data	Remarks
OBI50 optical televiewer.	Boremap lithological contact and fracture locations.	Length differences between core and image were collected, a function computed, and length values of image and natural gamma logs were recalculated in WellCAD.
ABI40 Acoustic televiewer.	Optical image, fractures, lithological contacts, driller´s data from oriented drilling (Devico), casing, bottom of borehole.	Length differences between optical and acoustic images were collected, length values were recalculated in WellCAD.
Natural gamma.	OBI50 natural gamma was used as length reference after image length correction.	The standalone gamma probe was broken, no separate measurements done. Instead the corresponding tool combined with gamma-gamma density was used for logging and length correction.
Gamma-gamma density.	Top and bottom length of logging, position of borehole casing, position of natural gamma anomalies compared to the one joined with separate OBI50 position of anomalies in optical image and corresponding features in Boremap lithology log.	Natural gamma data included in the gamma-gamma density logging tool was applied. Length differences between the two natural gamma logs were collected, length values of natural gamma and gamma-gamma density were applied the same recalculation in WellCAD.
Magnetic susceptibility.	Top and bottom lengths of logging, position of borehole casing, anomalies observed in density logging as compared to length already corrected OBI50 optical image, and corresponding features in Boremap lithology log.	Gamma-gamma density data and optical image data were used when correlating the length of susceptibility geological features. Differences were collected and length values recalculated in WellCAD.
DLL3 Dual laterolog.	Bottom of logging, casing, fractures, lithological contacts were used as length reference for matching.	DLL is more detailed than Elog (more fractures seen to correlate). Logging without bridle helps in upper part, used to control the separate logging in dry borehole, carried out with bridle. Differences were collected and length values recalculated in WellCAD.
Elog Resistivity and IP.	Bottom of logging, fractures, casing, comparison to more precise DLL3 profile were used as length reference for matching.	Differences to DLL and fractures were collected and length values recalculated in WellCAD.
Full waveform sonic.	Top and bottom, casing, fractures, lithological contacts, density and resistivity were used for length references.	Differences to reference length values were collected and length values recalculated in WellCAD.
Fluid temperature and conductivity.	Fluid temperature and logging was carried along with FWS and same length correction was used for both.	Measured together with FWS. Same adjustment was used to recalculate length values.

Gamma-gamma counts were re-computed to density values using a third degree polynomial fit made between recorded density data from petrophysical samples and tool count distribution in the same borehole. Density levels were adjusted so that lowest densities correspond to 2 650 kg/m^3 of fine-grained granite, higher densities in other rock types would also fall in range, and the median and modes of probability plot would coincide in both data sets. The purpose of re-calibration was to obtain geologically realistic density levels, and to normalize to the effect of the decaying ^{137}Cs source between different logging runs in previously measured borehole K03009F01. The source decay (30.4 years half-life) with time is not taken into account in the calibration, though this is a factor which could be compensated for by computing and tracking the decay for a specific source. Calibration is also specific to each borehole diameter.

Susceptibility calibration results were referred to nominal values of the calibration ring and air. A linear relation was derived. Level shift in the results was corrected so that the lowest values in low susceptibility intervals correspond to the level 500 micro-SI obtained by petrophysical analysis from the same borehole. This was necessary because the electromagnetic device measuring susceptibility has significant drift in recorded values. Also, the borehole diameter, conductivity of water filling and the temperature will affect the absolute level of the results. There remain some differences in the

calibrated logging data and petrophysical values even after computing compensation based on the values in calibration block and in the air, and using the petrophysical calibration data. One reason for this may be the differences in volume susceptibility and surface based measurement in samples and in the borehole.

The distribution of susceptibility data was compared with the distribution of petrophysical values. Because there was a difference at the high end of values, the susceptibility ranges were adjusted so that the logging and petrophysical values would conform. Adjustment was carried out by multiplying the calibrated logging data values with an experimental factor 1.5, based on examination of data distribution of petrophysics and logging. The likely reason for this ratio is survey geometry (volumetric susceptibility vs. contact measurement) and borehole effects.

The likely reason for the difference between calibrated susceptibility and petrophysical data are differences in borehole and sample geometry and volumes (magnetization), as well as the borehole diameter, water filling and probe geometry. Any other logging data than the density and the susceptibility was not readjusted according to the petrophysical sample data. Natural gamma does not include petrophysical analysis. Measured results are depending greatly on the structure and electronics of the probe and the detector, as well as the diameter and filling of the borehole, and the probe being centralized or not during the logging. Borehole geometry and probe centralisation related errors are within 3–5 % of the count rate when borehole diameter is 76 mm (Hallenburg 1984). These effects cannot be compensated for without carrying out separate measurements in a known medium and for the actual borehole geometry, which was not part of the scope of this work.

Resistivity and sonic logging are considered to provide physical property information of the medium, so that the tool calibrations and decisions regarding the interpretation and geometric compensations for borehole diameter (stand-off) are adequate to ensure representativity of the data.

4.4.3 Post-processing of other logging data

The natural gamma radiation sensor included in the gamma-gamma density probe is factory calibrated to API (American Petroleum Institute) units. This calibration is tool-independent and is removing the effects of crystal size, tool housing, and tool electronics. The calibration does not, however, remove the effects of borehole diameter and water content in the borehole, nor due to any temperature related drift of the tool readings.

Calibration is carried out at the University of Houston, in a calibration pit made of concrete. The concrete is made up of three layers, each 8 inches thick, of which the top and bottom layers are of very low radioactivity, and the middle layer is approximately twice as radioactive as typical midcontinent shales of the United States of America, the layer containing 13 ppm uranium, 24 ppm thorium and 4 % of potassium. Recording is carried out in a 5 ½ inch cased borehole. The gamma ray API unit is defined as 1/200 of the difference between the count rate recorded by a logging tool in the middle of the radioactive layer and that recorded in the middle of a non-radioactive layer (Hallenburg 1984).

The API values were further converted to micro-Röntgen per hour values using conversion factor 7.2 API = 1 μR/h (Schön 1995, Bradel 1985).

Fluid conductivity data were recalibrated using values from 13 KCl solutions of different electrical conductivity (EC) to derive a log-log 3rd-degree polynomial relationship. Fluid temperature measurement uses factory calibration settings. Fluid conductivity was compensated from measurement temperature to 25 °C using a conversion algorithm (Heikkonen et al. 2002) and a corresponding apparent TDS value was computed.

Dual laterolog resistivity was referred to measured resistor block values. A log-log ratio of measured and nominal values was derived as a 3rd degree polynomial. Measured data were adjusted according to this polynomial. The adjustment was intended to correct the recorded values to correspond to true resistivity levels. This adjustment does not take into account any effect of borehole diameter, tool construction or electrical conductivity of water in borehole. Comparison with normal resistivity data and petrophysical sample data from the same borehole has suggested that the dual laterolog results

are not nearly as much sensitive to the borehole geometry and fluid related differences as the normal logging results. Borehole effects are small for boreholes having a diameter less than 0.3–0.4 m, but corrections can be made for DLL measurements (Vasvári 2011, Schlumberger 1998). Order of magnitude of borehole effect corrections in DLL for 76 mm boreholes and high contrast between borehole water and bedrock are in order of 1.2–1.3 of the measured reading (Crain 2015).

Because one of the measurements was carried out in the water filled borehole, and severely affected by metallic objects attached to the probe, such borehole effect compensations are not useful here. The borehole effects in a dry hole repeated measurement are even less apparent for the shallow laterolog reading. The deep reading is affected by poor grounding, and differences between deep and shallow profiles suggest that compensation may be useful. Resistivity in Laterolog deep profile is possibly unrealistically high.

Normal resistivity was referred to measured resistor block values. A log-log ratio of measured and nominal values was derived as a 3rd degree polynomial. Measured data were adjusted according to this polynomial. The adjustment was intended to correct the recorded values to correspond to true resistivity levels. This adjustment does not take into account any effect of borehole diameter, tool construction or water in borehole.

The electrical conductivity of the water in the borehole as well as the diameter of the borehole significantly reduces the measured resistivity values compared to the bulk resistivity of the bedrock. The effect is stronger the shorter the electrode spacing, the higher the electrical conductivity of the water, and the larger the diameter of the borehole. There has been advised a recalibration procedure taking into account the resistivity of the water and borehole diameter (Dakhnov 1959), which was not attempted in this work because of spuriously low level of the normal logging data due to the metallic connecting piece on the top of the tool. The normal resistivity data, taking into account the erroneous level of resistivity, will nevertheless indicate the location of electrically more significant intervals in the borehole, especially those which are of larger dimension, when comparing with the laterolog data.

Full waveform sonic measurements consisted of wave forms (amplitude versus time) measured at four distances between transmitter and receiver (0.6 m, 0.8 m, 1.0 m and 1.2 m). Amplitude data were resampled in ReflexW software using a 0.5 microsecond time step. Resampling was carried out with linear interpolation of data points in the time domain. It may be more accurate to fit the actual waveform to the recorded data set. Semblance analysis of the arrival times of different wave fronts was computed using the four measured channels. The semblance analysis is producing amplitude vs. time log, where amplitude's low and high values indicate arrival times of different seismic P-, S- and Stoneley waves through the bedrock.

The tool construction of four receivers and one source (6 kHz strong transducer) can be used for semblance analysis based velocity interpretation. Picking of P- and S- onsets does not contain information on the correct phase, so the actual velocity level has to be estimated on the basis of semblance data, time differences between channels, and performance of standoff correction to adjust borehole diameter and acoustic velocity in the borehole fluid. Full waveform sonic apparently benefitted from pressurising the borehole by water filling, because the amplitude levels were higher than observed for the corresponding log of the K03009F01 borehole.

WellCAD software was used to pick the arrival times from the image processed with Semblance analysis. Picking used the maximum amplitude in processed image. Arrival times were converted to seismic velocity values.

Amplitude maximum of sonic waveform for P- and S- waves was picked from the channels from different distances, and P- and S-wave attenuation was computed. Tubewave energy was computed using integration for the channels from different distances, and tubewave attenuation was computed from the energy values.

The semblance-based velocity definition was checked by picking P- and S-wave travel times from all channels, and computing these values to velocities over the measurement distance, using a stand-off correction which is taking into account the borehole and tool diameters, transmitter-receiver distances, and the approximate acoustic velocity in borehole water. The velocity was also estimated

on basis of the travel time differences between different distances, though this appeared to be noisy. The P-wave velocity was also checked against the results obtained from petrophysical sample analyses. Logging data median values fall within ±150 m/s of laboratory specimen values (lower values are found in the logging). Differences may be caused by near borehole effects, observation scale, stress field, directional effects (borehole inclination angle with respect to foliation), and different frequency ranges. Specimen are from non-broken rock mass, and the results derived from the borehole full wave sonic logging are including also the effect of average fracturing in the rock mass, where fractures are decreasing the acoustic velocity.

Using the length corrected gamma-gamma density values, and P- and S-wave velocity values, the dynamic rock mechanical parameters Young's Modulus, Shear Modulus, Bulk Modulus, Bulk Compressibility and Poisson's ratio were computed from the borehole data.

The acoustic televiewer image was imported to WellCAD, first without orienting the image. Missing traces were interpolated. Tool rotation data were smoothened with a median filter, and used together with tool marker direction to compute the rotational angle of the tool.

Using the rotation angle, it was possible to reorient the image so that the left edge would always be aligned to high side, and the middle of the image towards the down direction in the borehole.

The travel time image was centralised using maximum and minimum value limits close to the nominal borehole caliper (diameter 75.8 mm). Using the nominal diameter (75.8 mm) as a reference, an apparent fluid acoustic velocity profile at 5 m spacing was defined. This velocity value is not a correct one, but was used as a constant value to compute the caliper image, and caliper minimum, average and maximum. Amplitude minimum and maximum profiles were computed from the amplitude image.

The pressure releases, two accidental at 43.7 m and 56.0 m and several intentional between 0–43 m, caused a 0…+0.5 mm error in the caliper reading at that interval. Also, the increase in pressure between 43–98 m is affecting the absolute accuracy. Basically, the pressure release locations can be recognized, and it would be possible to remove these effects manually with some extra work. This was not considered necessary for the quality of the results as caliper data are useful for showing locations where borehole diameter is larger than nominal due to softer rock quality or presence of fractures. Maintaining a constant pressure during logging would help in attaining a better absolute accuracy than 0.3 mm.

Logging results were compiled to produce composite files containing lithology, fracture frequency, and different logging data: standard geophysical logging, sonic interpreted data, sonic derivative rock mechanical parameters, fluid conductivity, sonic full wave form images, and acoustic televiewer image. Sonic full waveform was produced from the measurement tool in three different versions: wide band image appropriate for velocity interpretation, tubewave plot suitable for tubewave energy computation, and a so-called chevron plot, which displays well the v-shaped ("chevron") reflections occurring at fracture locations. Also, surface wave mode arrivals are well displayed in the chevron plot.

4.5 Analyses and interpretations

Specific analyses of data were not carried out to other than those required to facilitate length matching, computation of physical quantities (parameters) and quality control.

Density and susceptibility interpretations contain reference data from tool calibration and petrophysical data. Both density and susceptibility probes are affected by variations in borehole diameter. Since the susceptibility tool is an electromagnetic device it exhibits a diurnal drift as well as a temperature drift, something that need to be manually compensated for. The density tool also shows decay of the ^{137}Cs source (some 3 % annually). These factors need to be taken into account in the final calibration.

Natural gamma was recorded simultaneously with gamma-gamma density. Values were calibrated by the manufacturer to American Petroleum Institute (API) unit levels. These values were subsequently converted to the unit micro Röntgen per hour.

Electrical measurements suffered a severe decrease in resistivity level due to the air hose connector being made of brass. Repeated run of measurements conducted in the dry borehole without the connector succeeded well for the Dual Laterolog logging using a shallow electrode spacing. The repeated run for the Deep electrode spacing was more spurious.

The semblance analysis appeared to produce overestimated and fairly inaccurate velocity levels when using original time sampling set to 4 microseconds. Resampling of the traces using a 0.5 micro-second time interval produced a much more precise accuracy, and more reasonable velocity levels. Semblance analysis uses the time differences between four channels, and is insensitive to poor centralisation of the tool, or differences in fluid velocity.

The above-mentioned trade-offs were resolved by using semblance analysis as the primary velocity information, and time picking derived amplitude for amplitude and attenuation data.

Borehole diameter profile can be interpreted from acoustic televiewer. This parameter is commonly called a “Caliper Log”. Interpretation is based on travel time of acoustic wave reflected from the wall of borehole. Absolute caliper readings cannot be obtained from the televiewer data without supporting information. The image needs to be computationally centralised within some limited range of values to avoid spurious caliper readings. Caliper readings are also strongly dependent on fluid temperature, salinity (affecting the fluid density and thus the velocity) and pressure. The effect of these parameters was mostly compensated for by editing an average fluid velocity profile using a nominal borehole diameter of 75.8 mm. Caliper results were then computed using a generalised fluid velocity curve.

The acoustic televiewer data were greatly improved compared to earlier results from nearly horizontal boreholes. This was attributed to the pressurizing of the borehole with water during measurement. Pressure increased during the measurement such that the water filling hose connector came accidentally loose twice during the measurement. This caused an evident 0.5 mm jump in the caliper readings at those positions and created some amplitude anomalies due to release of gas in the borehole fluid. Caliper values are smaller at higher pressure. Low amplitude is observed at short borehole sections due to gas bubbles which do not reflect the acoustic wave back. Low amplitude in these cases is found on high (upper) side of the borehole, as the light gas is located above the heavier water. The second pressure drop the pressure level was decreased gradually at a period of a few minutes. This caused a slight 0.3 mm variation in the caliper background level. In the future, it will be crucial to maintain a constant water pressure in the borehole using a check valve.

4.6 Nonconformities

Generally, the field work performed smoothly. Compared to the scheduled borehole measurement programme, some exceptions occurred, which are regarded as nonconformities.

The natural gamma radiation probe was broken when checked in the field. The tool was functional during a check before mobilisation. The production logging was replaced with a natural gamma sensor included within the gamma-gamma density probe. Due to smaller sodium-iodine (NaI) crystal size and shorter count integration time available, the sensitivity of the probe is lower than the separate ALT GRA probe.

Consequently, the borehole length reference between different logging runs (methods) was not possible with natural gamma logging as originally planned. Length reference had to be replaced with geological references and comparison of common features between different methods (Sigurdsson 2016). An exception here is the available optical televiewer (OBI50) logging data provided from SKB. The data included natural gamma logging. In the length matching procedure length matching for OBI50 data was first performed using fractures and lithology from Boremap. The length for OBI50 image and the natural gamma logging were adjusted according to this matching. Then the length of the gamma-gamma density log was matched with the adjusted natural gamma length from OBI50. The image from Acoustic Televiewer (ABI40) was matched with comparison with similar features in the OBI50 image.

Susceptibility, resistivity and full wave sonic length references were deduced using geological check points and common features between density-susceptibility, density-velocity, susceptibility-resistivity and resistivity-velocity. Fluid resistivity and temperature logging was run simultaneously with Full Waveform Sonic, and applied the same length adjustment.

The Elog resistivity and DLL values were affected by the metallic connector of the air hose and caused severely lowered resistivity values. DLL was re-measured in a dry borehole using a connector bridle and 10 m glass fiber push rod extension closest to the probe. This provided reasonably accurate and high resolution resistivity data from the borehole with dual laterolog shallow array. The dual laterolog deep profile contains spurious values apparently due to low electrical current level (poor grounding in dry borehole).

The resistivity level of normal resistivities is very low because of the metallic object near the probe. The normal resistivity logging was not repeated in the dry borehole. Normal resistivity logging commonly involves a correction for effects of fluid electrical conductivity and borehole diameter. Because the results are strongly erroneous in level, these corrections were rejected. Sections with low resistivity, due to fractures and deformation zones, are visible in the data despite of lower level of background.

The caliper results computed from acoustic televiewer data have sudden minor level changes due to release of water pressure, which happened twice completely and several controlled releases (which were not recorded). Pressure release intervals also indicate gas bubbles in the image (low reflectivity towards the high side of the borehole, towards the direction indicating vertically upward in a horizontally oriented borehole).

No other nonconformities occurred during field work or processing.

5 Results and discussion

The geophysical logging results are presenting physical parameters in profiles along the borehole. The parameters and their combinations describe the lithological variation, alteration, intensity of fracturing and an indication of ductile and brittle deformation. The location data on fracturing will also assist in identifying the hydraulically significant fractures or deformation zones. An indication of that the borehole K08028F01 intersects larger deformation zones can´t be find, but the indication of the presence of minor deformation zones and their evidence can be assessed from the data.

1. Rock type variation is described by gamma-gamma density, susceptibility and natural gamma logging. The main rock types in Äspö have typically different density levels. Susceptibility is also varying between the rock types. Together the density and susceptibility assist in classifying the rock types as granite, granodiorite or diorite-gabbro. This is caused by the iron content (magnetite, hematite and pyrite or pyrrhotite) in the rock forming silicate minerals. The proportion of highly magnetized magnetite or pyrrhotite minerals is shown by elevated susceptibility with respect to the density. In Äspö the natural gamma radiation is elevated in fine grained granite and some variants of granodiorite, which makes it possible to further differentiate between rock types. Rock types more mafic in composition have low levels of natural gamma radiation.

   The seismic P- and S- wave velocities are partly associated with rock type, diorite-gabbro having clearly elevated velocity compared to other rock types. Similarly, the resistivity is partly (via texture and porosity) linked with rock type variation.

2. Fracture frequency is described as an overprint of typical rock type associated values in electrical resistivity and seismic velocities. Both are lowered by increased fracture frequency. Isolated fault cores or significant fractures show distinct minima in velocity and resistivity profiles. The fluid temperature and resistivity profiles show also changes (high and low values and gradients) due to open or possibly hydraulically conductive fractures. Acoustic televiewer is a good tool to detect almost all types of fractures, and practically almost every fracture in the borehole.

3. Alteration and deformation change the properties of the rock compared to unaltered rock mass of the same (or original) lithology. The most significant effects of alteration observed in this borehole are a complete decay of magnetization compared to the density level (formation of hematite), increase of acoustic velocity in epidotized rock mass when non fractured (lack of porosity), and more likely varying degree of decrease in resistivity and seismic velocities in and near the deformation zones, which may emerge from change in mineral composition (clay alteration), occurrence of micro fractures or elevated porosity, and occurrence of fractures.

4. Potentially hydraulically conductive fractures and fracture zones are associated with aperture seen in acoustic televiewer amplitude image, and increased caliper in travel time image. The hydraulically conductive fractures may also cause changes in temperature and water salinity profile. Rarely a washout in clay- or grain-filled fractures may be seen as a gamma-gamma density minimum. More likely is to observe water filled fractures as distinct minima in resistivity and in seismic velocity. Water filled fractures also act as sources of tube waves traveling upward and downward along the borehole, starting from the given fracture location.

A list of discovered geological features is shown in Table 5-1.

Table 5-1. Indications of lithology, fracturing, deformation zones and hydraulic conductivity obtained from the geophysical logging results.

Length interval	Mapped geology	Lithology indication	Fracturing indication	Deformation zone indication	Hydraulic conductivity indication
0–2 m.	Casing.				
2–4.3 m.	Fine-grained granite.	Low density, average susceptibility, increased natural gamma radiation.	One resistivity minimum.	Average or slightly reduced seismic velocities, slightly lowered resistivity.	One resistivity minimum.
4.3–31.47.	Ävrö granodiorite.	Average density and susceptibility.	Slightly lowered resistivity, clear resistivity minima at 5.25 m, 6.23 m, 11.45 m, 13.56 m, 15.53 m, 16.29 m, 17.16 m, 18.25 m, 20.02 m, 20.59 m, 21.96 m, 23.53 m (low sonic velocity), 31.44 m (low sonic velocity).	Fine-grained granite occurrences, mostly elevated susceptibility, one at 26–27 m has low susceptibility and high natural gamma radiation and slightly lowered velocity, increased velocity at 12–17 m.	Possibly significant fracture at 31.44 m due to low sonic velocity. Temperature and salinity changes at 19.17–21.2 m and 30.07 m.
31.47–39.90 m.	Fine-grained granite.	Low density at 32–35 m, average susceptibility at 35–40 m, low susceptibility and partly high natural gamma radiation. Elevated elastic moduli at 30–32 m.	Resistivity and velocities are varying. Distinct minimum in both resistivity and sonic velocity at 37.64 m.	Average resistivity and sonic velocity. Susceptibility elevated at lower contact (40 m).	Possibly significant fracture at 37.64 m due to low resistivity and sonic velocity.
39.90–57.53 m.	Ävrö granodiorite (Äspö diorite at 42.40–44.80 m).	Average density, average susceptibility though highly varying, average natural gamma radiation. Fine-grained diorite-gabbro has low susceptibility.	Slightly lowered sonic velocity. Average or slightly elevated resistivity. At 43–51 m several indications of fractures due to decreased resistivity. Indications of fractures at 44, 49, 51.2, 55.6, 60.3 m, due to decreased velocity.	Epidotization of fine-grained diorite-gabbro is visible as low susceptibility.	Potential significant fractures at 43 m, 47.8 m, 51.17 m due to decreased resistivity.
57.53–66.29 m.	Ävrö granodiorite (59.49–62.97 m fine-grained granite).	Low density, average and varying susceptibility, elevated natural gamma radiation. Average sonic velocity.	Fracture indications due to decreased resistivity and decreased velocity at 60.4, 63.0 m.	In places low susceptibility values compared to elevated density levels.	
66.29–70 m.	Fine-grained diorite-gabbro.	Elevated density and velocity, variable or high resistivity, low natural gamma radiation and low susceptibility. High elastic moduli.	Fracture indications due to decreased resistivity at 67.75 m, 69.21 m, 69.91 m.	In places low susceptibility values compared to elevated density levels.	Possibly significant fractures at 69.21 and 69.91 m due to decreased resistivity. Temperature variations.
70–76 m.	Ävrö granodiorite.	Average density, average susceptibility, average natural gamma radiation, average resistivity and average velocities. Pegmatite intersection shows elevated natural gamma radiation.	No fracture indications.	No deformation indications.	No indications of significant fractures. Changes in salinity at 76.17 m.

Length interval	Mapped geology	Lithology indication	Fracturing indication	Deformation zone indication	Hydraulic conductivity indication
76–79.85 m.	Fine-grained granite.	Low density, average and varying susceptibility, elevated natural gamma radiation (high at 76.7 m), variable and in places elevated resistivity and velocities.	Indication of fracturing at 78.8 m due to reduced resistivity.	No support for an indication of a deformation zone.	Possible fracture at 78.8 m due to decreased resistivity.
79.85–84.71 m.	Ävrö granodiorite.	Average density, moderately to low susceptibility, elevated and varying natural gamma radiation, average resistivity and sonic velocities.	Fracture indications at 81.33 m and 83.15 m due to reduced resistivity.	No support for an indication of a deformation zone.	Possible fracture at 81.33 m and 83.15 m due to reduced resistivity.
84.71–88.44 m.	Fine-grained diorite-gabbro.	High density, high velocity, variable resistivity. Completely loss in susceptibility, low natural gamma radiation. At contact 87.7–88.44 m high natural gamma radiation, low density. High elastic moduli at 85–87 m.	Indications of fractures at 84.7, 85.3, 86.37, 86.9 m, due to reduced resistivity.	Very low susceptibility compared to elevated density level, indicating the possibly magnetized minerals have lost their magnetization, vanished or altered to another mineral (magnetite to hematite, for example).	Indication of possibly more significant fractures at 84.7 and 85.3 m, due to reduced resistivity.
88.44–90.18 m.	Fine-grained diorite-gabbro.	Elevated density, very low susceptibility, low resistivity, low sonic velocity. Average natural gamma radiation.	Fracture indications due to reduced resistivity and reduced velocity.	Very low susceptibility, low resistivity and low velocity.	Fracture indications due to reduced resistivity and reduced velocity at 88.87 and 89.55 m.
90.18–94.38 m.	Ävrö granodiorite.	Average density, average natural gamma radiation, very low susceptibility, low resistivity and low velocity. Low elastic moduli.	Fracture indications due to reduced resistivity and reduced velocity.	Very low susceptibility, low resistivity and velocity.	Strong indications at 90.13, 90.93 and 91.89 m, due to reduced resistivity and reduced velocity.

Fluid temperature and electrical conductivity vary within a small range. Noted minor changes in temperature and water resistivity indicate locations of fractures producing groundwater flow in to or out of the borehole. Fluid electrical conductivity (and hence salinity) is high due to high amounts of total dissolved solids. This affects the resistivity level of the electrical resistivity logs (mostly the normal resistivity logs).

Acoustic televiewer (ABI) data show some variation in caliper values. Increased caliper values can be associated with fractures or rock of reduced quality. Increased caliper values can also be related to drilling technical issues like slip of the break ring in the drill bit, or by manually focused drill bit rotation generated by the driller at certain depth levels. Markings caused by steered drilling at 64.86–66.04 m and 72.78–74.05 m (Nilsson 2015) are visible in ABI caliper and amplitude data.

Density is governed by the iron content of the rock forming minerals (silicate density). In highly porous rock types, or fractured rock with fractures of large aperture or soft infillings (fault gouge), the water content may provide some decreasing contribution to the density. Granites typically show the lowest densities of the intact rocks, with a successibly increasing density seen for granodiorites, diorites and gabbros, respectively. The density in K08028F01 shows a rather small deviation with overall median values of around 2.7 g/cm^3. The highest density values are obtained where the borehole transect Äspö diorite and gabbroid rocks.

Magnetic susceptibility is also associated with minerals containing iron. Susceptibility values fall in the paramagnetic low susceptibility range with dependency on density, or the clearly elevated ferrimagnetic range, indicating significant content of magnetite or pyrrhotite. The noted susceptibility range on basis of the logging data in K08028F01 and the petrophysical sample analysis from the same borehole indicates that the rock mass has a fairly high susceptibility, suggesting elevated magnetite content. In some intervals alteration has probably lowered the susceptibility significantly (resulting in low susceptibility).

Electrical resistivity logging shows both rock texture and porosity related bulk resistivity, which to some extent is related to the rock type, and the presence of fractures and deformation zones, which have a decreasing effect on resistivity. Presence of saline water tends to amplify this effect. Alteration may have either decreasing or sometimes even increasing effect on resistivity. Occurrence of electrically conductive minerals (pyrite, pyrrhotite, sphalerite, clay) on fracture coatings or within the intact rock also affects resistivity. The focused dual laterolog data represent fairly well the resistivity level and provides a tool for comparing resistivities between boreholes. It also contributes to the precise localization of open or filled fractures, and shows some deformation zone with elevated fracture frequency and possible damages in intact rock masses also around the actual deformation zones.

The electrical resistivity logging with dual laterolog array in this borehole was carried out at dry borehole conditions. The Dual Laterolog Shallow and Deep profiles (shorter and longer current electrode spacing) were functioning differently even though simultaneously recorded. The electrical grounding of the longer electrode spacing was not good enough and consequently the injected current was too low to obtain high resolution data, and hence some spurious results were recorded. The Dual Laterolog Shallow profile is more representative of true resistivity data than the Deep profile in this borehole. Because the shallow and deep profiles are intended to be used together to assess the effect of groundwater salinity in the bedrock, it will be better to make the logging in water filled borehole in future. This will require removing metallic objects from vicinity of active electrodes.

The single point resistivity (SPR) combined with the normal resistivity tool is measuring contact resistance on the borehole wall. Normal resistivity at increasing electrode distances indicate increasing trend when rock mass shows a higher resistivity than the resistivity of the borehole fluid. Larger electrode distances represent deeper and less disturbed rock mass because the current is spreading into a larger volume of the rock around the borehole. It is also less affected by the electrical conductivity of the water in the borehole.

In crystalline bedrock, the effect of drilling induced damage (EDZ) near the borehole is negligible compared to the effect of EDZ in sedimentary rocks. Typically, different spacing in configuration of the resistivity normal arrays can be used to evaluate the significance of the detection of deformation zones. Extensive deformation zones are causing stronger resistivity anomalies for the longer

electrode spacing, whereas the small deformation zones, e.g. isolated fractures, are best or only seen in the shorter electrode spacing data. Normal resistivity arrays can thus indicate differences between smaller (or shorter) fractures and larger (or longer) fractures. The latter (large fractures) often have a core in the centre of the deformation zone and damage zone where increased porosity in the rock mass and elevated fracture frequency around the deformation zone core affect the resistivity level around the deformation zone and in the surrounding bedrock. The resistivity level of resistivity normal logging is strongly affected by the borehole groundwater electrical conductivity.

Induced polarization effect is associated with mineral content and grain size. Certain minerals, i.e. iron containing minerals, have high, and some others like clay low IP. Fairly small IP values and minor variations were encountered in borehole K08028F01.

Full waveform sonic contains information of elastic wavefield in the rock mass near the borehole. The resulting images show variation in arrival times, amplitudes, and different kind of diffracted and reflected energy. Wideband images (classical full waveform presentation) indicate the P- and S-wave and tubewave arrivals, and show up- and downgoing tubewaves generated at the intersection between the borehole wall and the fractures. They also indicate v-shaped reflected P- and S-waves for some fractures. Tubewave images show high frequency surface wave ringing and amplitude along borehole wall. High amplitudes of tubewaves is associated with open fractures intersecting the borehole wall. The low frequency chevron plot indicates strong reflections from fractures. It seems to display also surface wave modes which are travelling backward and forward along the borehole wall from the actual location of the fracture or deformation zone intersecting the borehole.

Interpretation on the basis of different waveforms results in interpreted P- and S- wave velocities, amplitudes and attenuations. The velocities depend on texture and mineral content of the rock types. They are also strongly affected by porosity and the frequency of open fractures. Deformation zone locations show distinct velocity minima. Some higher velocity veins or rock type intersections are also met, for example epidote bearing, possibly altered rock, and dioritic-gabbroic rock. Amplitude seems to carry information on lithology and fracturing. Attenuation of amplitude is associated with brittle deformation and fracturing. Lower tubewave energy levels and computed higher attenuation are associated with fracturing of the rock.

Dynamic rock mechanical parameters (Young's Modulus, Shear Modulus, Bulk Modulus, Bulk Compressibility and Poisson's ratio) computed from P- and S-wave velocities and bulk densities are indicating apparent levels and variations in rock strength, associated with rock textures, e.g. lithological characteristics and grade of deformation. The obtained profiles can serve to supplement laboratory data on discrete samples with information from continuous geophysical logs, though levels of data are by definition different in dynamic and static conditions. The dynamic values computed from seismic velocities and densities are almost always higher than the static values measured with elastic deformation from laboratory specimen by rock mechanical testing.

This is due to fact that the acoustic sound wave for dynamic measurements finds the quickest path through the volume of rock through mineral grain boundaries, whereas the elastic deformation for a static measurement, e.g. within a rock specimen in a laboratory will indicate any failure in the grains and their boundaries. The more deformed the rock mass is, the larger is the difference between dynamic (in situ) and static (laboratory specimen) data. Actual dependency and ratio between the dynamic and static data is site specific and its lithology and it cannot be exactly known without comparison of the derived moduli between the different measuring conditions. The dynamic moduli profiles from geophysical logging constitute the only possibility to estimate rock mechanical parameters for the deformation zones, as laboratory specimen analysis require non-broken samples which are seldom possible to achieve in practice.

Statistics based on the acquired results are given in Table 5-2. Complete data are stored in the SICADA database and are also presented in Appendices as WellCAD plots in the attached data disc. The WellCAD Reader program is also included in the data disc.

Table 5-2. Survey methods, logging intervals and univariate statistics.

Method (unit)	Top depth (m)	Bottom depth (m)	Min	Max	Median	Average	Standard deviation	No of samples
Fluid temperature (°C)	1.67	93.46	12.9	14.3	13.2	13.2	0.17	4560
Fluid Electrical conductivity (S/m)	1.67	93.46	0.26	1.67	1.51	1.50	0.10	4560
Fluid Electrical conductivity at 25 °C (S/m)	1.67	93.46	0.33	2.20	1.98	1.96	0.13	4560
TDS (g/l)	1.67	93.46	1.77	12.89	11.45	11.35	0.84	4560
Caliper average ABI (mm)	1.18	92.62	73.49	103.53	75.95	76.01	0.45	59299
Susceptibility ($1E^{-5}$ SI)	0.68	94.40	−5.0	51340	1481	2040	5344	4687
Natural Gamma Radiation (µR/h)	0.01	93.01	1.568	57.459	22.367	23.371	7.646	4635
Density (g/cm^3)	1.06	94.24	2.42	3.56	2.70	2.71	0.10	4644
Dual Laterolog Shallow (Ωm)	1.16	93.27	1.6	26712	14528	13658	7157	4581
Dual Laterolog Deep (Ωm)	1.16	92.83	1.8	231666	40599	56856	47289	4559
Single Point Resistance (Ω)	0.27	93.12	4.4	928.4	343.0	340.8	68.1	4633
Normal Resistivity 8” (Ωm)	0.16	93.50	0.9	3353.8	840.5	837.3	199.6	4654
Normal Resistivity 16” (Ωm)	0.06	93.50	1.3	3464.0	1459.1	1441.0	299.4	4659
Normal Resistivity 32” (Ωm)	0.01	93.49	0.5	3059.2	2366.4	2320.9	472.3	4661
Normal Resistivity 64” (Ωm)	0.01	93.95	0.1	7117.4	2094.0	2055.9	403.5	4634
IP effect Ma (ms)	0.06	94.60	3.20	50048.10	10.07	37.08	770.69	4717
Sonic P Velocity (m/s)	1.75	93.03	5409	6258	5779	5796	109	4562
Sonic S Velocity (m/s)	1.75	93.03	2817	3633	3381	3383	91	4562
Sonic P amplitude 0.6 m	1.74	93.63	−206	1117	157	213	148	4585
Sonic P amplitude 1.2 m	1.74	93.61	−113	1097	97	100	49	4584
Sonic S amplitude 0.6 m	1.74	93.61	−1336	3518	1531	1487	512	4584
Sonic S amplitude 1.2 m	1.74	93.61	−271	1397	646	626	210	4584
Sonic P attenuation (dB/m)	1.73	93.61	−45.7	90.3	6.5	9.6	10.7	4595
Sonic S attenuation (dB/m)	1.73	93.61	−78.1	56.6	12.6	12.4	6.6	4595
Sonic Tubewave Energy 0.6 m	1.72	93.61	2521	184387	6188	28116	41729	4585
Sonic Tubewave Energy 1.2 m	1.72	93.61	443	109489	1756	11727	19555	4585
Sonic Tubewave Attenuation (dB/m)	1.72	93.61	−27.7	35.6	17.80	17.98	6.39	4585
Poisson’s ratio	1.76	93.02	0.17	0.34	0.24	0.24	0.02	4561
Young’s modulus (GPa)	1.76	93.02	55.7	97.1	76.3	76.9	4.53	4547
Shear Modulus (GPa)	1.76	93.02	20.7	39.9	30.8	31.0	2.00	4547
Bulk Modulus (GPa)	1.76	93.02	39.3	66.2	49.1	49.7	3.35	4547
Bulk Compressibility (1/GPa)	1.76	93.02	0.015	0.025	0.02	0.02	0.001	4547

6 Concluding remarks

Geophysical borehole logging field work in K08028F01 went smoothly. Full coverage of logging with all planned methods except natural gamma radiation was obtained. Measurements in upward inclined borehole with sealing system to maintain water in the borehole during survey was advised and this was performed for the first time. Work in new pressurized conditions performed well.

Some development is still required for the electrical resistivity measurement technique. All metallic objects near the active electrodes need to be removed or properly sealed. Compensation of borehole water electrical conductivity and borehole diameter was not performed due to erroneously low resistivity values in the data, which mean that corrections would not have produced improved results either.

Maintaining constant pressure during measurement will be useful at least for acoustic televiewer and full waveform sonic logging. Acoustic televiewer got much benefit of pressurized borehole conditions, though varying pressure affected the travel time values (and thus caliper).

Using natural gamma logging as length reference was not possible due to tool failure. The procedure of using natural gamma logs in all tools was replaced by using geological reference points obtained from core logging with Boremap (Sigurdsson 2016) and comparison of common features in the core logging was used for correlation with different methods.

In the future, the natural gamma logging should be included in all borehole logging runs when possible.

Field work timing in a 100 m long upwards inclining borehole with 0.02 m spacing of data storage and 1–3 m/min logging speed allows approximately two, maximum three logging runs each day. Survey and preparations together took three and a half working days to perform. The logging operation included six borehole logging runs and two repeat runs.

Work in upward inclined boreholes is possible when the borehole sealing device is used and the borehole is filled with water. The majority of the time is used for filling and emptying the borehole with water. Most of the logging methods require water filled boreholes and at least calibration is only possible to perform when water is present. Possibilities to optimize the time of the field work rely on attaching several probes together in the same borehole run. Centralised full wave sonic, fluid temperature and resistivity and acoustic televiewer may be joined together with some limitations (acoustic televiewer and fluid temperature and resistivity both need to be the lowermost probes), as well as non-centralised resistivities, susceptibility, density and natural gamma logging may be joined together with similar restrictions (susceptibility and density both need to be lowermost probes).

References

SKB's (Svensk Kärnbränslehantering AB) publications can be found at www.skb.com/publications.

Bradel E, 1985. Bohrlochgeophysik. In Bender F (ed). Angewandte Geowissenschaften. Bd. 2, Methoden der angewandten Geophysik und mathematische Verfahren in den Geowissenschaften. Stuttgart: Enke. (In German.)

Crain E R, 2015. Crain's petrophysical handbook (CPH). Available at: https://www.spec2000.net

Dakhnov V N, 1959. Promyslovaia geofizika. Moskva: Gostopekh-Izdat. (English translation (part) by G.V. Keller 1962, Geophysical well logging. Quarterly of the Colorado School of Mines 57, 445.

Hallenburg J K, 1984. Geophysical logging for mineral and engineering applications. Tulsa, OK: Penwell Books.

Heikkonen J, Heikkinen E, Mäntynen M, 2002. Pohjaveden sähkönjohtavuuden lämpötilakotj auksen matemaattinen mallinnus synteettisten vesinäytteiden mittauksista [Mathematical modelling of temperature adjustment algorithm for groundwater electrical conductivity on basis of synthetic water sample analysis]. Posiva Working Report 2002-10, Posiva Oy, Finland. (In Finnish.)

Komulainen J, Pöllänen J, 2016. KBS-3H – DETUM. Difference flow logging in boreholes K03009F01 and K08028F01. SKB P-15-13, Svensk Kärnbränslehantering AB.

Nilsson G, 2015. Steered core drilling of boreholes K03009F01 and K08028F01 at the Äspö HRL. Deliverable D-No:D4:05, LUCOEX project, European Commission. (Also published as SKB P-15-11, Svensk Kärnbränslehantering AB).

Schlumberger, 1998. Log interpretation charts. SMP-7006, Schlumberger Wireline & Testing. Sugar Land, Texas.

Schön J (ed), 1995. Handbook of geophysical exploration. Section 1, Seismic exploration, Vol. 18. Physical properties of rocks: fundamentals and principles of petrophysics. Oxford: Pergamon.

Sigurdsson O, 2016. KBS-3H. Boremap mapping of K08028F01. SKB P-15-14, Svensk Kärnbränslehantering AB.

Vasvári V, 2011. On the applicability of dual laterolog for the determination of fracture paramters in hard rock aquifers. Austrian Journal of Earth Sciences 104/2, 80–89.

Appendix 1

Review of appendices

The following appendices are included in this report:

2. Field activity time log.
3. Petrophysical data from samples.

Following appendices and associated data are included in WellCAD and pdf files stored on the data disc:

4. Geophysical Properties.

   (Files named as:
   App4_K08028F01_StandardGeophysicalLogs.pdf and
   App4_K08028F01_StandardGeophysicalLogs.wcl).

   – Lithology (Rock type, rock type < 1m, alteration type, alteration intensity).
   – Fracture frequency.
   – Caliper, average, ABI measurement.
   – Gamma-gamma density.
   – Density (petrophysics).
   – Magnetic susceptibility.
   – Magnetic susceptibility (petrophysics).
   – Chargeability (Ma).
   – Natural gamma radiation.
   – Resistivity, Dual laterolog shallow.
   – Resistivity, Dual laterolog deep.
   – Resistivity (petrophysics).
   – Single point resistance.
   – Normal resistivity, 8”.
   – Normal resistivity, 16”.
   – Normal resistivity, 32”.
   – Normal resistivity, 64”.
   – S-wave velocity.
   – P-wave velocity.
   – P-wave velocity(petrophysics).

5. Fluid Properties.

   (Files named as:
   App5_K08028F01_FluidLogs.pdf and
   App5_K08028F01_FluidLogs.wcl).

   – Lithology (Rock type, rock type < 1m, alteration type, alteration intensity).
   – Fracture frequency.
   – Caliper, average, ABI measurement.
   – Fluid temperature.
   – Total dissolved solids (TDS).
   – Fluid electrical conductivity, in situ –temperature (Fluid EC (T)).
   – Fluid electrical conductivity, corrected to 25 °C (Fluid EC (25 °C)).
   – Resistivity, Dual laterolog deep (Resistivity DLL Deep).
   – S-wave velocity.

6. Acoustic Hole Imaging.

   (Files named as:
   App6_K08028F01_ABI40_toHigh_scale20.pdf and
   App6_K08028F01_ABI40_toHigh.wcl).

   – Amplitude.
   – Caliper image, half caliper.
   – Caliper minimum.
   – Caliper maximum.
   – Caliper average.
   – Amplitude minimum.
   – Amplitude maximum.
   – 3D image of the borehole.

7. Rock Mechanical Properties.

   (Files named as:
   App7_K08028F01_RockMechanicalLogs.pdf and
   App7_K08028F01_RockMechanicalLogs.wcl).

   – Lithology (Rock type, rock type < 1m, alteration type, alteration intensity).
   – Fracture frequency.
   – Caliper, average, ABI measurement.
   – Gamma-gamma density.
   – S-wave velocity.
   – P-wave velocity.
   – Poisson's ratio.
   – Shear modulus.
   – Young's modulus.
   – Bulk modulus.
   – Bulk compressibility.
   – Full Waveform Sonic.

8. Full Waveform Sonic.

   (Files named as:
   App8_K08028F01_SonicLogs.pdf and
   App8_K08028F01_SonicLogs.wcl).

   – Lithology (Rock type, rock type < 1m, alteration type, alteration intensity).
   – Fracture frequency.
   – Caliper, average, ABI measurement.
   – P-wave amplitude, 0.6 m.
   – P-wave amplitude, 1.2 m.
   – S-wave amplitude, 0.6 m.
   – S-wave amplitude, 1.2 m.
   – P-wave attenuation.
   – S-wave attenuation.
   – Tubewave energy, 0.6 m.
   – Tubewave energy, 1.2 m.
   – Tubewave attenuation.

9. Full Waveform Sonic, wideband log.

   (Files named as:
   App9_K08028F01_FWS_wideband.pdf and
   App9_K08028F01_FWS_wideband.wcl).

   – Lithology (Rock type).
   – Fracture frequency.
   – Caliper, average, ABI measurement.
   – Full waveform sonic, 0.6 m wide band (RX1-1A-Wide Band).
   – Full waveform sonic, 0.8 m wide band (RX2-1A-Wide Band).
   – Full waveform sonic, 1.0 m wide band (RX3-1A-Wide Band).
   – Full waveform sonic, 1.2 m wide band (RX4-1A-Wide Band).

10. Full Waveform Sonic, chevron plot.

    (Files named as:
    App10_K08028F01_FWS_chevron.pdf and
    App10_K08028F01_FWS_chevron.wcl).

    – Lithology (Rock type).
    – Fracture frequency.
    – Caliper, average, ABI measurement.
    – Full waveform sonic, 0.6 m chevron plot (RX1-1A-Chevron).
    – Full waveform sonic, 0.8 m chevron plot (RX2-1A- Chevron).
    – Full waveform sonic, 1.0 m chevron plot (RX3-1A- Chevron).
    – Full waveform sonic, 1.2 m chevron plot (RX4-1A- Chevron).

11. Full Waveform Sonic, tubewave plot.

    (Files named as:
    App11_K08028F01_FWS_tubewave.pdf and
    App11_K08028F01_FWS_tubewave.wcl).

    – Lithology (Rock type.)
    – Fracture frequency.
    – Caliper, average, ABI measurement.
    – Full waveform sonic, 0.6 m tubewave (RX1-1A-Tube).
    – Full waveform sonic, 0.8 m tubewave (RX2-1A-Tube).
    – Full waveform sonic, 1.0 m tubewave (RX3-1A-Tube).
    – Full waveform sonic, 1.2 m tubewave (RX4-1A-Tube).

Appendix 2

Field activity time log

Table A-2. Time log of field activities.

Date	Start time	End time	Activity	Notes
2014-08-25	11:00		Arrival to Äspö site.	
	11:30		Site introduction.	
	14:00		Move tools to site.	Leaving to site temperature.
	15:00		Push rod rig introduction.	
	15:30		Drive from the site.	
	16:00	17:00	Joining air hose 50 + 50 m at base.	
2014-08-26	07:45		Drive to the site.	Access card not valid, had to wait for fixing.
	07:50		Open water valve. Start nitrogen gas bubbling of water in the tank.	
	08:10		Borehole empty.	
	08:15	09:30	Mounting of sealing device.	
	09:30	10:45	Checking and calibrating Elog IP and Resistivity and Natural Gamma Radiation probes.	Gamma probe is broken and cannot be used with any tool as length reference. Calibration with resistor box ok.
	10:45	11:10	Elog Normal Resistivity and IP to end of borehole.	Operating with push rod rig, last meter manually.
	11:10	11:20	Push rods out.	
	11:20	11:50	Sealing borehole collar.	
	11:50	12:05	Feeding water.	
	12:05	13:05	Lunch break.	
	13:05	13:17	Feeding water.	
	13:17	13:40	Air hose out.	
	13:40	14:30	ELOG IP and Normal Resistivity logging.	ALT Bbox. Winch driven logging backward towards collar. No bridle, return current grounded to tunnel floor with fixed electrode. Results are badly lowered in resistivity level because of brass connector for push rod and air hose.
	14:30	14:50	Water out of hole.	
	14:50	15:25	Check DLL probe. DLL probe to end of borehole.	Operating with push rod rig.
	15:25	15:40	Push rods out.	
	15:40	16:30	Water in.	Approximately 400 litres.
	16:30	16:35	Air hose out.	
	16:35	17:15	DLL logging out.	ALT Bbox. Winch driven logging backward towards collar. No bridle, return current grounded to tunnel floor with fixed electrode. Results are badly lowered in resistivity level because of brass connector for push rod and air hose.
	17:15	17:25	Borehole empty.	
	17:25	17:40	Calibrate DLL.	Calibration with resistor box ok.
		17:40	Close valve.	
		17:50	Drive from the site.	

Date	Start time	End time	Activity	Notes
2014-08-27		7:20	Open valve, start nitrogen gas bubbling of water in the tank.	
		7:30	Borehole water away.	
		08:10	ABI probe to the end of the borehole.	Operating with push rod rig, 8 m/min.
		08:30	Push rods out.	
		08:35	Borehole closed.	
		09:05	Borehole full.	Approximately 400 litres.
		09:15	Air hose out, borehole sealed.	
	09:15	11:15	Acoustic Televiewer logging.	Winch driven logging backward towards collar. Interrupted winch run during lunch break. Pressure lost at 65 m and 43 m due to loose valve and connector. Clear effect on travel time results.
	11:15	12:15	Lunch break.	
	12:15	13:12	Acoustic Televiewer.	Pressure manually released frequently to avoid damage.
		13:40	Water out.	
	14:10	15:30	Push rod machine out of order.	Fixed by Pierre Nilsson.
	14:10	15:10	DLL resistivity logging 0–30 m.	Testing in dry hole. Surprisingly good results.
		15:50	Density probe to the end of borehole.	Operating with push rod rig, 8 m/min.
		16:00	Push rods removed from borehole.	
		16:50	Borehole filled with water.	Approximately 400 litres.
	17:00	17:50	Gamma-gamma density logging.	Winch driven measurement upwards. No problems in data retrieval. Simultaneous natural gamma.
		18:00	Borehole empty.	
		18:05	Valve closed.	

Date	Start time	End time	Activity	Notes
2014-08-28		07:14	Valve open, nitrogen gas bubbling of water in the tank.	Water collected in the tank, surplus left to drain.
		07:25	Borehole empty.	
	07:35	07:45	DLL to the end of the borehole.	Glass fiber rods, manual pushing.
	07:55	08:30	DLL logging.	Dry borehole. Winch driven logging backwards to the collar. Push rods removed during logging. Bridle connector was manually hoisted over the encoder wheel when ending. During last meters the bridle grounded into moist tunnel floor with stainless steel electrode.
	08:35	08:40	Susceptibility calibration.	Calibration values stored in file with tool being two days at in situ temperature. Measured in air, with hand kept on tool, and with magnetic block.
		09:10	Susceptibility probe to end of borehole.	Operated with push rod rig.
		09:30	Push rods out.	
		10:10	Borehole full, air hose out.	
	10:10	11:00	Susceptibility logging.	Winch driven measurement backwards to the collar of borehole.
	11:00	11:15	Susceptibility calibration.	Second calibration recorded with probe in air, with hand kept on, and with magnetic block.
	11:00	11:15	Water out of borehole.	
		12:15	Lunch break.	
		12:55	Full wave sonic probe to the end of borehole.	Operated with push rod rig. Last meter manually. Very heavy to move even by three persons.
		13:15	Rods out.	
		13:50	Borehole full, air hose out.	Sealing borehole.
		15:40	Full wave sonic and fluid resistivity logging.	Wireline logging upwards. Data storage at 4 microsecond interval until 4 000 microsecond. Connected fluid temperature and resistivity probe functioned well with backward direction.
		16:10	Water out.	
		16:10	Valve closed.	Borehole groundwater pressure gauge fixed.
2014-08-29		07:15	Valve open, nitrogenate tank.	Pressure in the borehole has increased to 30 bar overnight.
		07:30	Water away.	
		07:56	FWS to the end of borehole.	
		08:08	Push rods out.	
		08:17	Borehole closed.	
		08:50	Water filled.	Pressure max 15 bar.
		08:54	Air hose out.	
		10:13	FWS logging.	Extended mode to 16 ms time, 20 ms sampling, channel RX3 to obtain reflections. Works well. Pressure 5–15 bar.
		10:24	Water out.	
		10:35	Close valve.	
		10:50	Leave site.	Field project complete.
		14:00	Leave Äspö HRL.	Delivery of raw data.

Appendix 3

Petrophysical data from samples

Table A-3. Petrophysical data from K08028F01. Frequency effect of induced polarization was measured from low frequency (0.1 and 10 Hz, PL) and high frequency (10 Hz and 500 Hz, PT).

No.	Start depth (m)	End depth (m)	Density (kg/m^3)	Susceptibility (10^{-6} SI)	Remanence (10^{-3} A/m)	Seismic P wave velocity (m/s)	Resist-ivity (Ωm) 0.1Hz	Resist-ivity (Ωm) 10Hz	Resist-ivity (Ωm) 500Hz	IP (%) PL	IP (%) PT	Porosity (%)	Lithology (sample)
1	3.85	3.90	2632	14815	148	6099	36300	34200	31600	6	13	0.35	Fine-grained granite
2	6.85	6.90	2726	32655	316	5931	13200	15600	13900	0	0	0.36	Ävrö granodiorite
3	12.80	12.85	2676	28048	34	5932	29300	27400	24100	6	18	0.31	Deformed Ävrö granodiorite
4	15.70	15.75	2718	14855	182	6116	22800	21500	18200	6	20	0.42	Ävrö granodiorite
5	17.65	17.70	2746	17490	172	5932	15900	15100	13600	5	14	0.45	Ävrö granodiorite
6	30.20	30.25	2733	19143	60	5860	14500	13800	12100	5	17	0.54	Ävrö granodiorite
7	35.09	35.14	2664	17177	127	6057	73100	67900	54700	7	25	0.25	Fine-grained granite
8	38.87	38.93	2660	3438	144	5950	24800	23300	21100	6	15	0.50	Fine-grained granite
9	40.77	40.82	2723	14800	40	5952	22600	21400	18600	5	18	0.46	Ävrö granodiorite
10	50.42	50.47	2658	26361	36	5920	18000	17000	15600	6	14	0.47	Fine-grained granite
11	51.33	51.38	2658	26326	112	5915	52100	49100	42700	6	18	0.35	Fine-grained granite
12	54.65	54.70	2736	19138	139	6041	17900	16900	15400	5	14	0.42	Ävrö granodiorite
13	60.75	60.80	2638	7351	129	5776	17600	17200	16300	2	8	0.78	Fine-grained granite
14	61.45	61.50	2655	20566	116	5838	21200	20400	18700	4	12	0.56	Fine-grained granite (darker)
15	63.73	63.78	2658	12905	123	5723	8450	8160	7670	3	9	0.75	Ävrö granodiorite (foliated)
16	67.23	67.28	2919	673	146	6068	53800	50300	40200	7	25	0.18	Fine-grained diorite-gabbro
17	67.96	68.01	2919	642	55	6196	47400	44200	37000	7	22	0.16	Fine-grained diorite-gabbro
18	68.88	68.93	2936	616	141	6313	69200	64300	50500	7	27	0.14	Fine-grained diorite-gabbro (more fractures)
19	72.27	72.32	2706	11377	75	5915	16600	16000	14700	4	11	0.62	Ävrö granodiorite
20	77.55	77.60	2651	7086	108	5942	5980	6010	5790	0	2	0.67	Fine-grained granite
21	78.55	78.60	2647	13612	81	5956	5700	5760	5540	0	2	0.69	Fine-grained granite
22	83.38	83.43	2748	6383	42	5836	11300	11000	10400	3	8	0.50	Ävrö granodiorite
23	84.85	84.90	2919	610	250	6448	14900	14200	13100	5	12	0.29	Fine-grained diorite-gabbro
24	86.77	86.82	2926	623	138	6389	8780	8600	8060	2	8	0.36	Fine-grained diorite-gabbro
25	89.57	89.62	2810	800	52	5327	343	394	388	0	0	2.48	Fine-grained diorite-gabbro (with veins)
26	91.58	91.63	2718	531	180	5882	3280	3380	3270	0	0	0.92	Ävrö granodiorite (deformed)
27	92.73	92.78	2745	682	154	5705	14000	13500	12500	4	11	0.48	Ävrö granodiorite (deformed)

Geophysical Properties

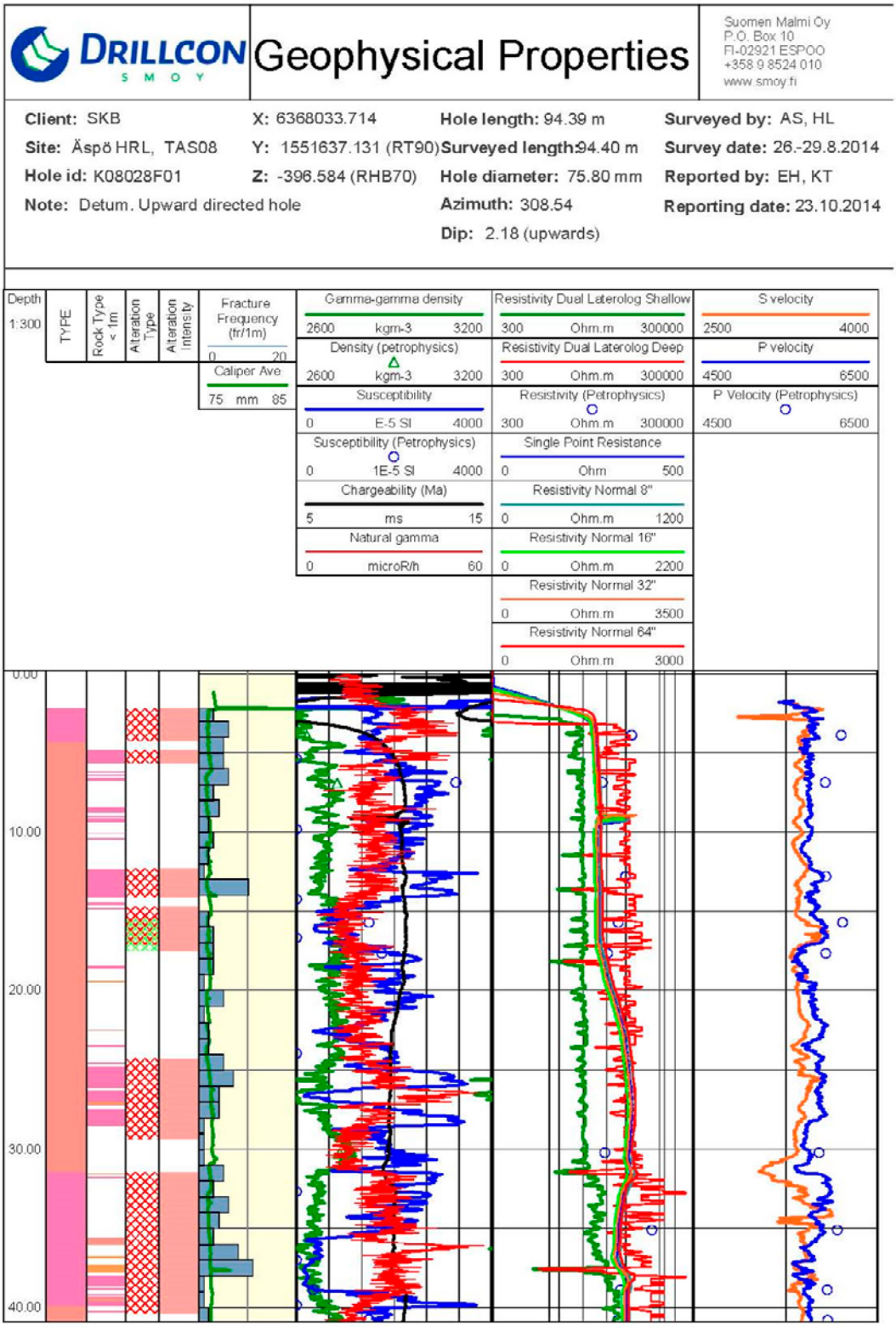

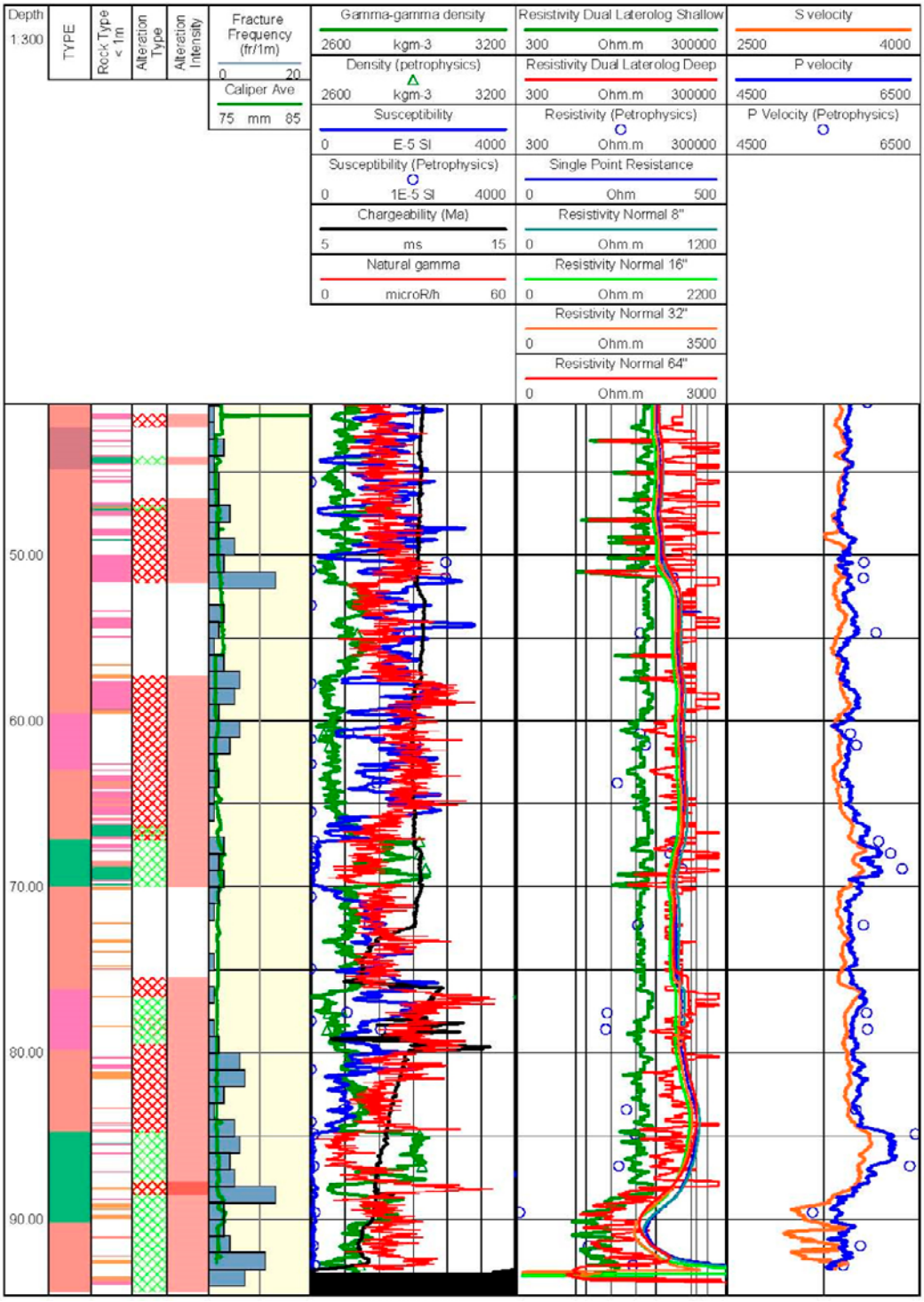
Depth
1:300
TYPE
Rock Type < 1m
Alteration Type
Alteration Intensity
Fracture Frequency (fr/1m)
0 20
Caliper Ave
75 mm 85
Gamma-gamma density
2600 kgm-3 3200
Density (petrophysics)
2600 kgm-3 3200
Susceptibility
0 E-5 SI 4000
Susceptibility (Petrophysics)
0 1E-5 SI 4000
Chargeability (Ma)
5 ms 15
Natural gamma
0 microR/h 60
Resistivity Dual Laterolog Shallow
300 Ohm.m 300000
Resistivity Dual Laterolog Deep
300 Ohm.m 300000
Resistivity (Petrophysics)
300 Ohm.m 300000
Single Point Resistance
0 Ohm 500
Resistivity Normal 8"
0 Ohm.m 1200
Resistivity Normal 16"
0 Ohm.m 2200
Resistivity Normal 32"
0 Ohm.m 3500
Resistivity Normal 64"
0 Ohm.m 3000
S velocity
2500 4000
P velocity
4500 6500
P Velocity (Petrophysics)
4500 6500
50.00
60.00
70.00
80.00
90.00

Fluid Properties

DRILLCON SMOY

Fluid Properties

Suomen Malmi Oy
P.O. Box 10
FI-02921 ESPOO
+358 9 8524 010
www.smoy.fi

Client: SKB
Site: Äspö HRL, TAS08
Hole id: K08028F01
Note: Detum. Upward directed hole

X: 6368033.714
Y: 1551637.131 (RT90)
Z: -396.584 (RHB70)

Hole length: 94.39 m
Surveyed length: 93.61 m
Hole diameter: 75.80 mm
Azimuth: 308.54
Dip: 2.18 (upwards)

Surveyed by: AS, HL
Survey date: 28.8.2014
Reported by: EH, KT
Reporting date: 28.10.2014

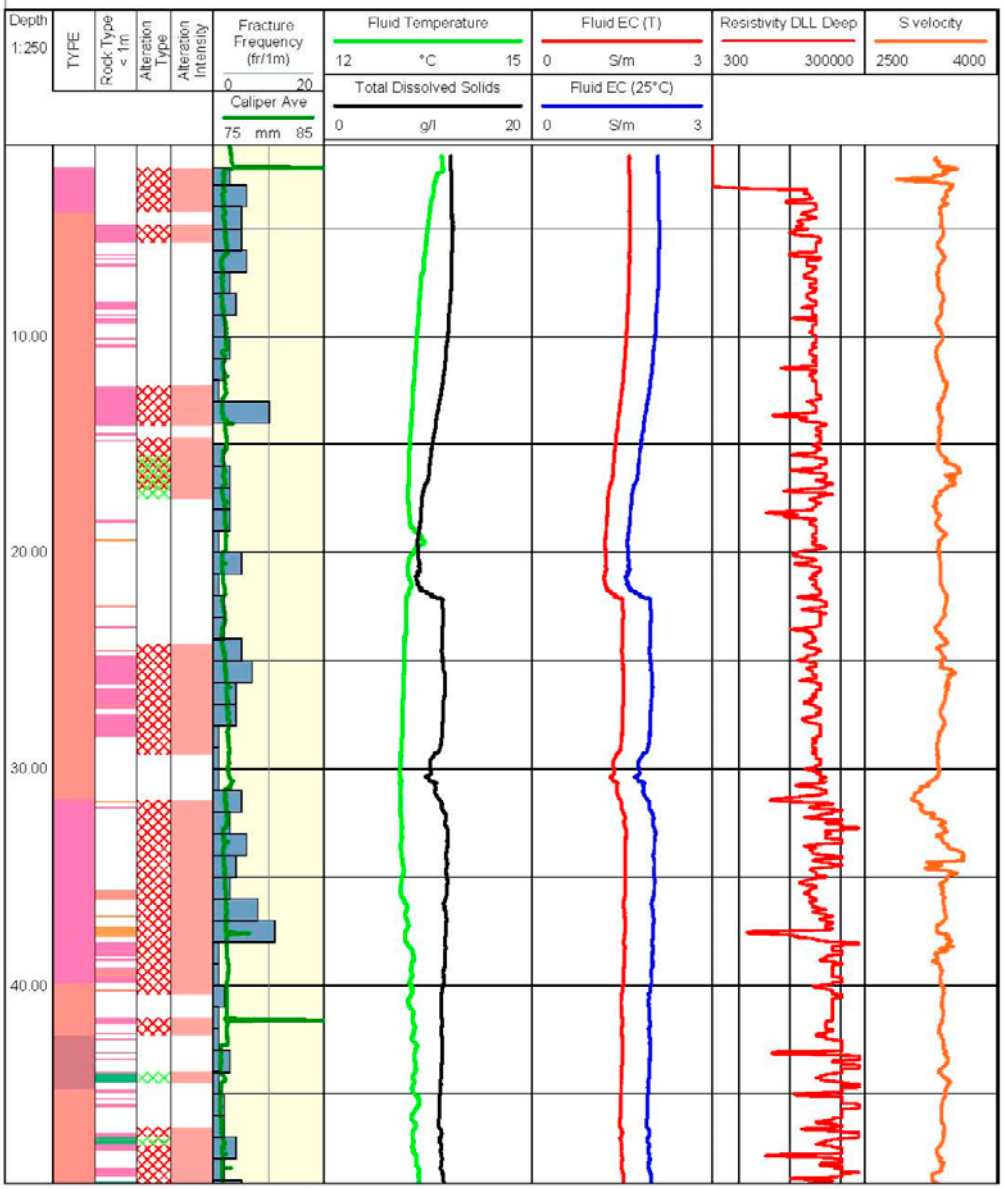

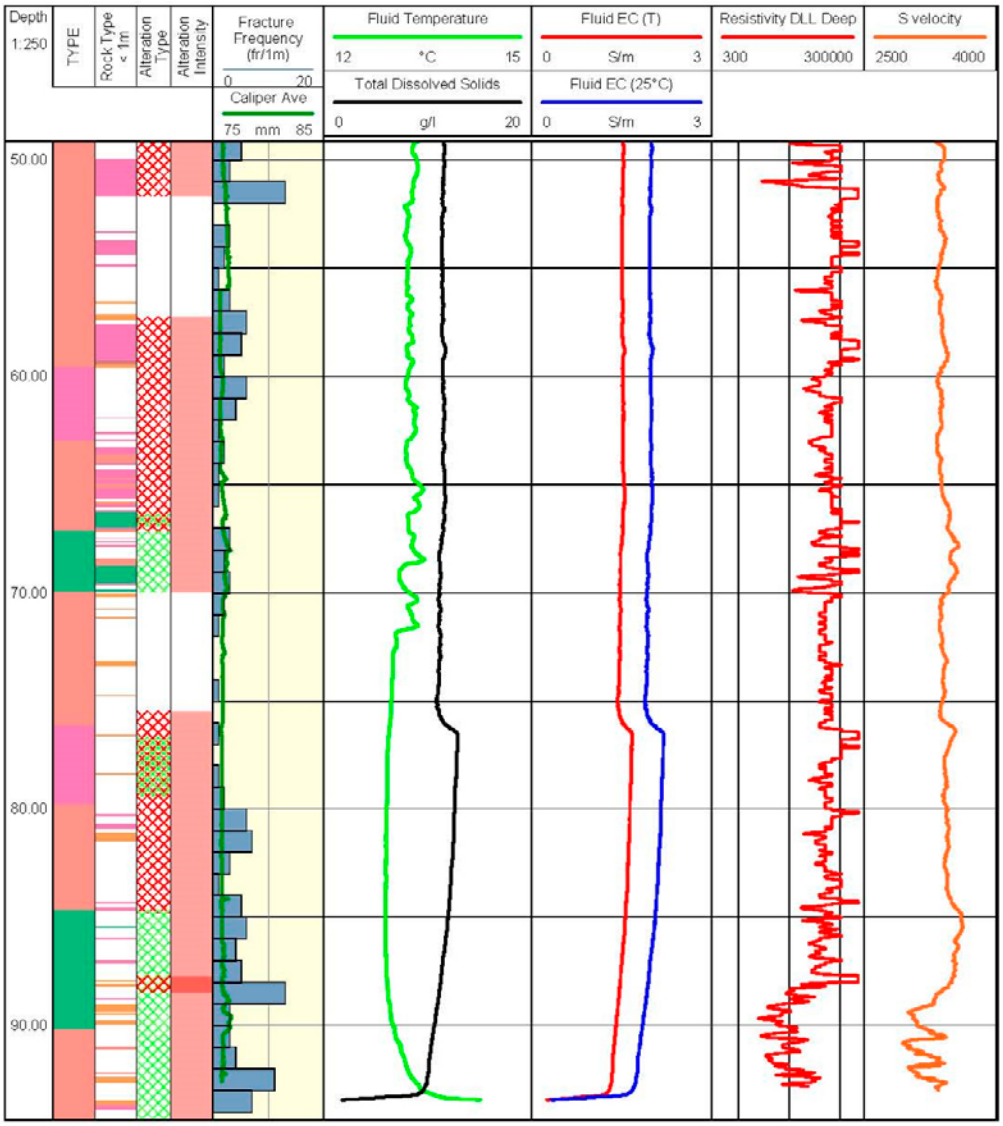
Depth
1:250
TYPE
Rock Type < 1m
Alteration Type
Alteration Intensity
Fracture Frequency (fr/1m)
0 20
Caliper Ave
75 mm 85
Fluid Temperature
12 °C 15
Total Dissolved Solids
0 g/l 20
Fluid EC (T)
0 S/m 3
Fluid EC (25°C)
0 S/m 3
Resistivity DLL Deep
300 300000
S velocity
2500 4000
50.00
60.00
70.00
80.00
90.00

Acoustic Hole Imaging

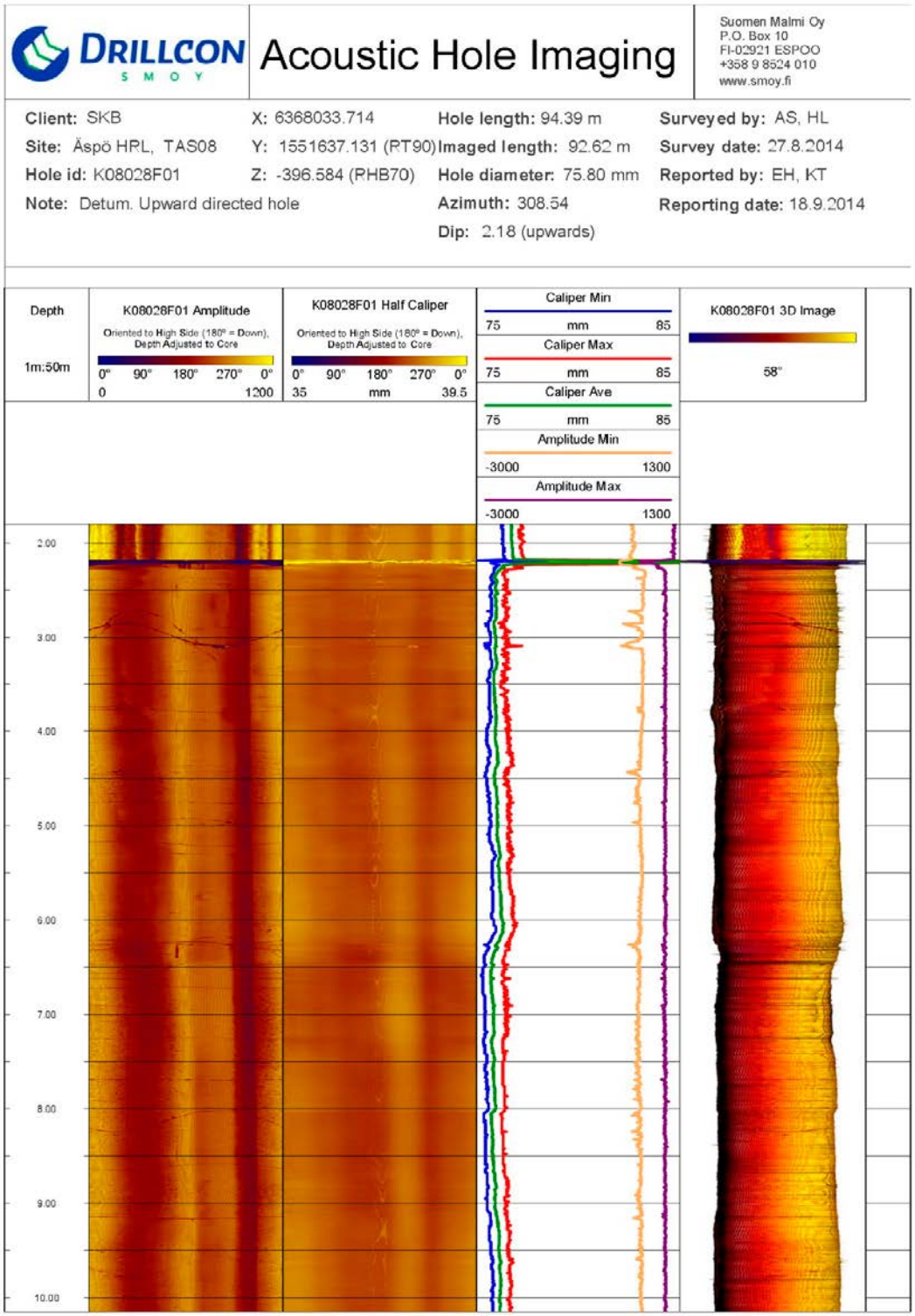

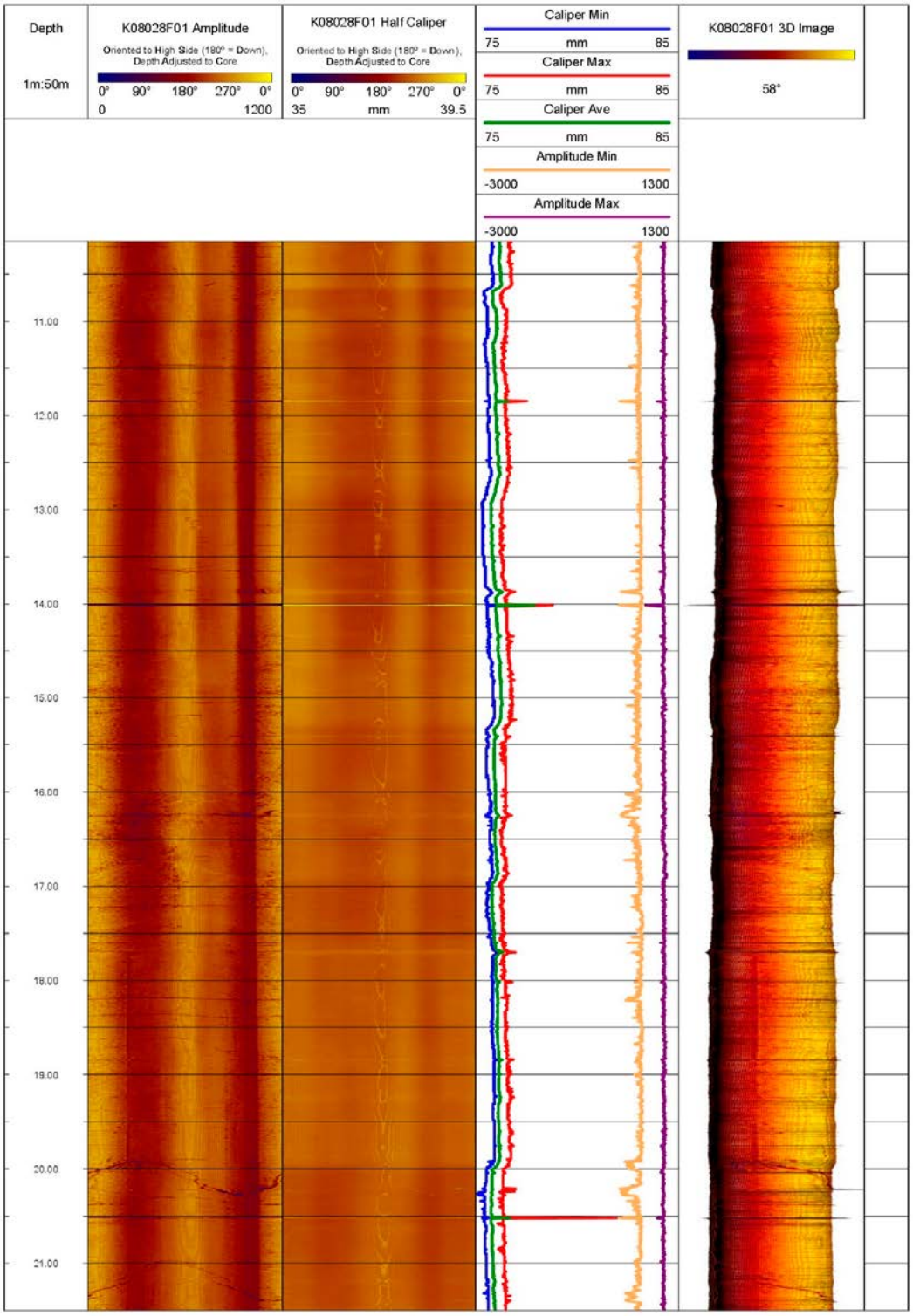
Depth
1m:50m
K08028F01 Amplitude
Oriented to High Side (180° = Down), Depth Adjusted to Core
0° 90° 180° 270° 0°
0
1200
K08028F01 Half Caliper
Oriented to High Side (180° = Down), Depth Adjusted to Core
0° 90° 180° 270° 0°
35
mm
39.5
Caliper Min
75
mm
85
Caliper Max
75
mm
85
Caliper Ave
75
mm
85
Amplitude Min
-3000
1300
Amplitude Max
-3000
1300
K08028F01 3D Image
58°
11.00
12.00
13.00
14.00
15.00
16.00
17.00
18.00
19.00
20.00
21.00

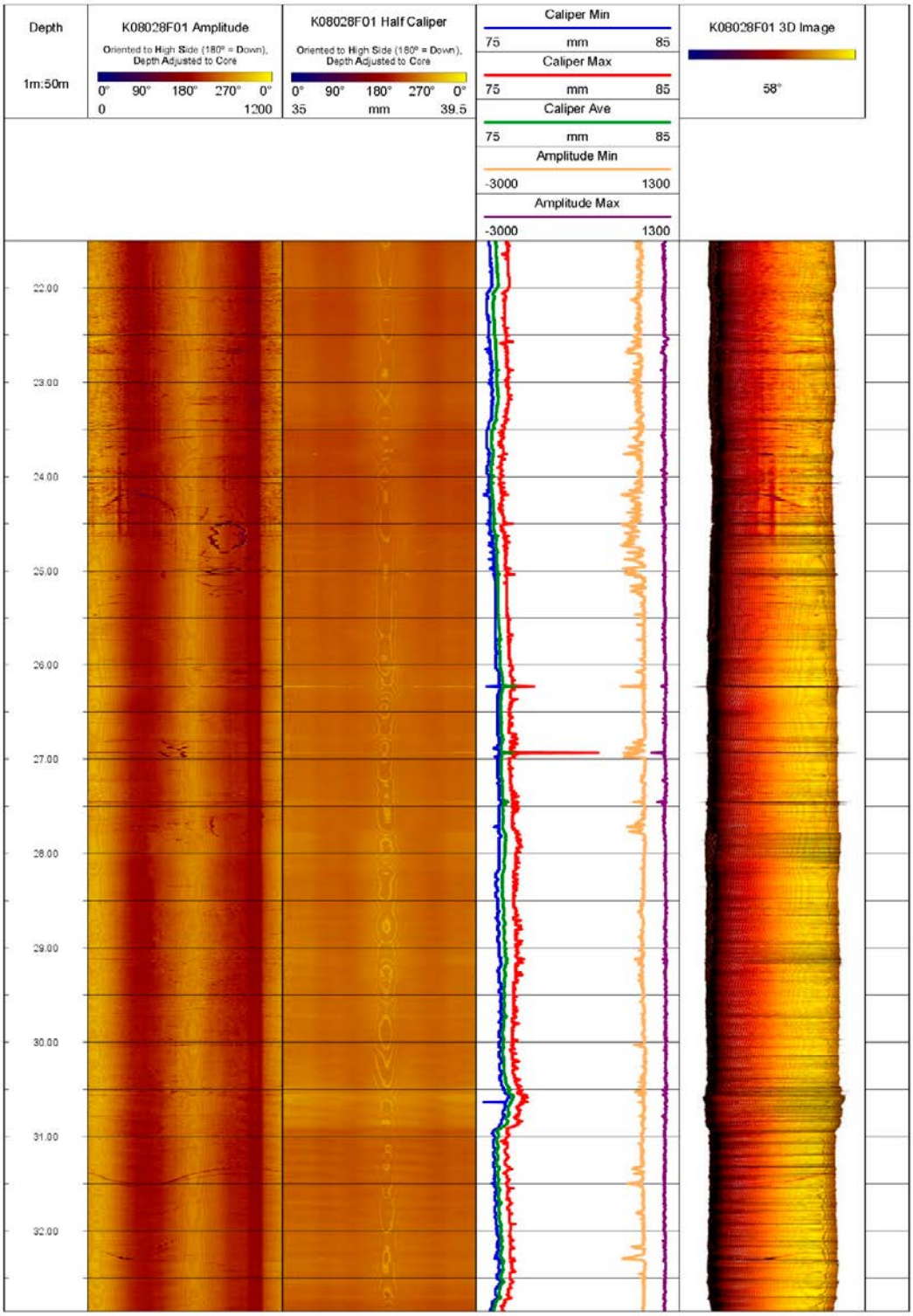
Depth
1m:50m
K08028F01 Amplitude
Oriented to High Side (180° = Down), Depth Adjusted to Core
0° 90° 180° 270° 0°
0
1200
K08028F01 Half Caliper
Oriented to High Side (180° = Down), Depth Adjusted to Core
0° 90° 180° 270° 0°
35
mm
39.5
Caliper Min
75
mm
85
Caliper Max
75
mm
85
Caliper Ave
75
mm
85
Amplitude Min
-3000
1300
Amplitude Max
-3000
1300
K08028F01 3D Image
58°
22.00
23.00
24.00
25.00
26.00
27.00
28.00
29.00
30.00
31.00
32.00

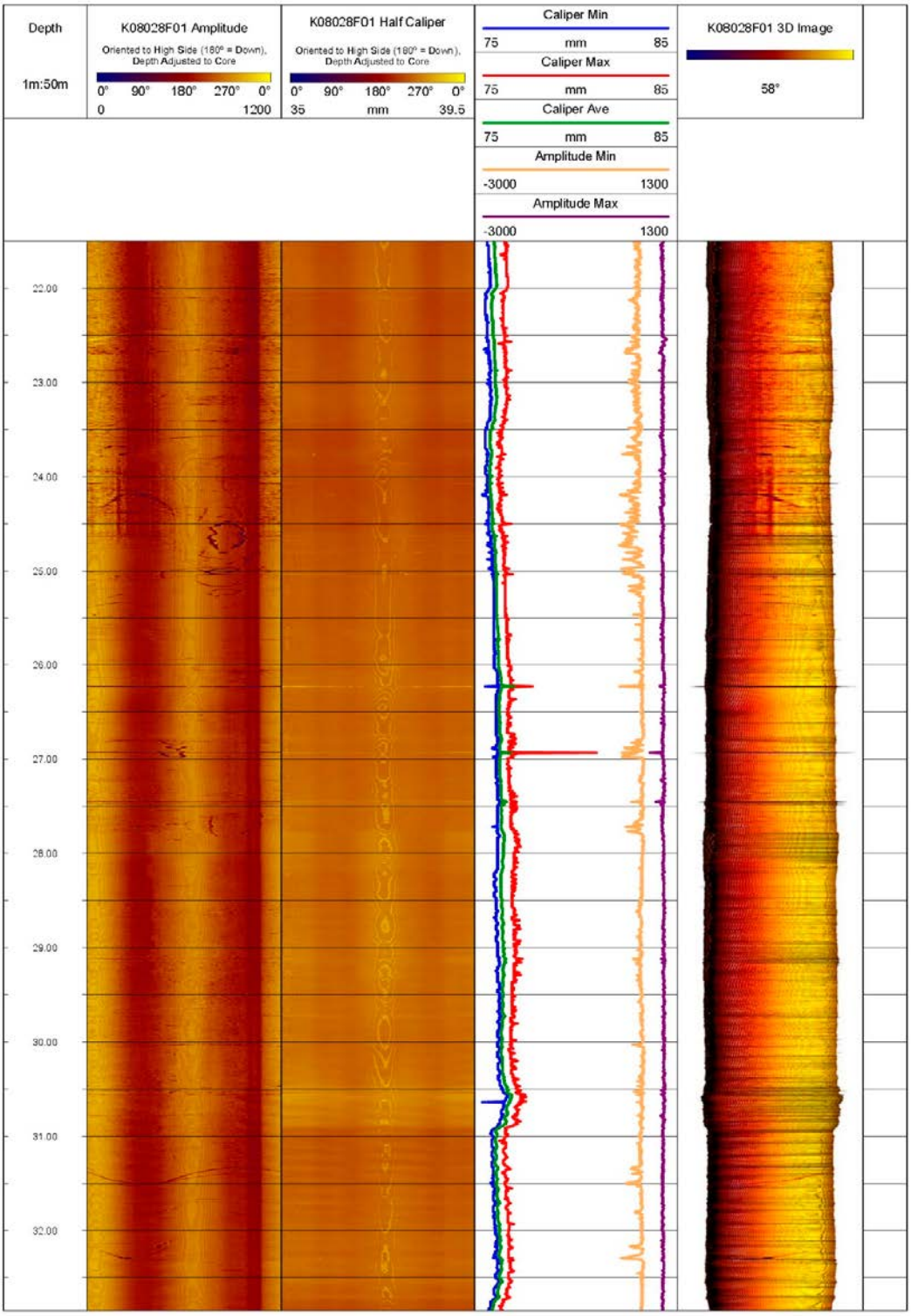
Depth
1m:50m
K08028F01 Amplitude
Oriented to High Side (180° = Down), Depth Adjusted to Core
0° 90° 180° 270° 0°
0 1200
K08028F01 Half Caliper
Oriented to High Side (180° = Down), Depth Adjusted to Core
0° 90° 180° 270° 0°
35 mm 39.5
Caliper Min
75 mm 85
Caliper Max
75 mm 85
Caliper Ave
75 mm 85
Amplitude Min
-3000 1300
Amplitude Max
-3000 1300
K08028F01 3D Image
58°
22.00
23.00
24.00
25.00
26.00
27.00
28.00
29.00
30.00
31.00
32.00

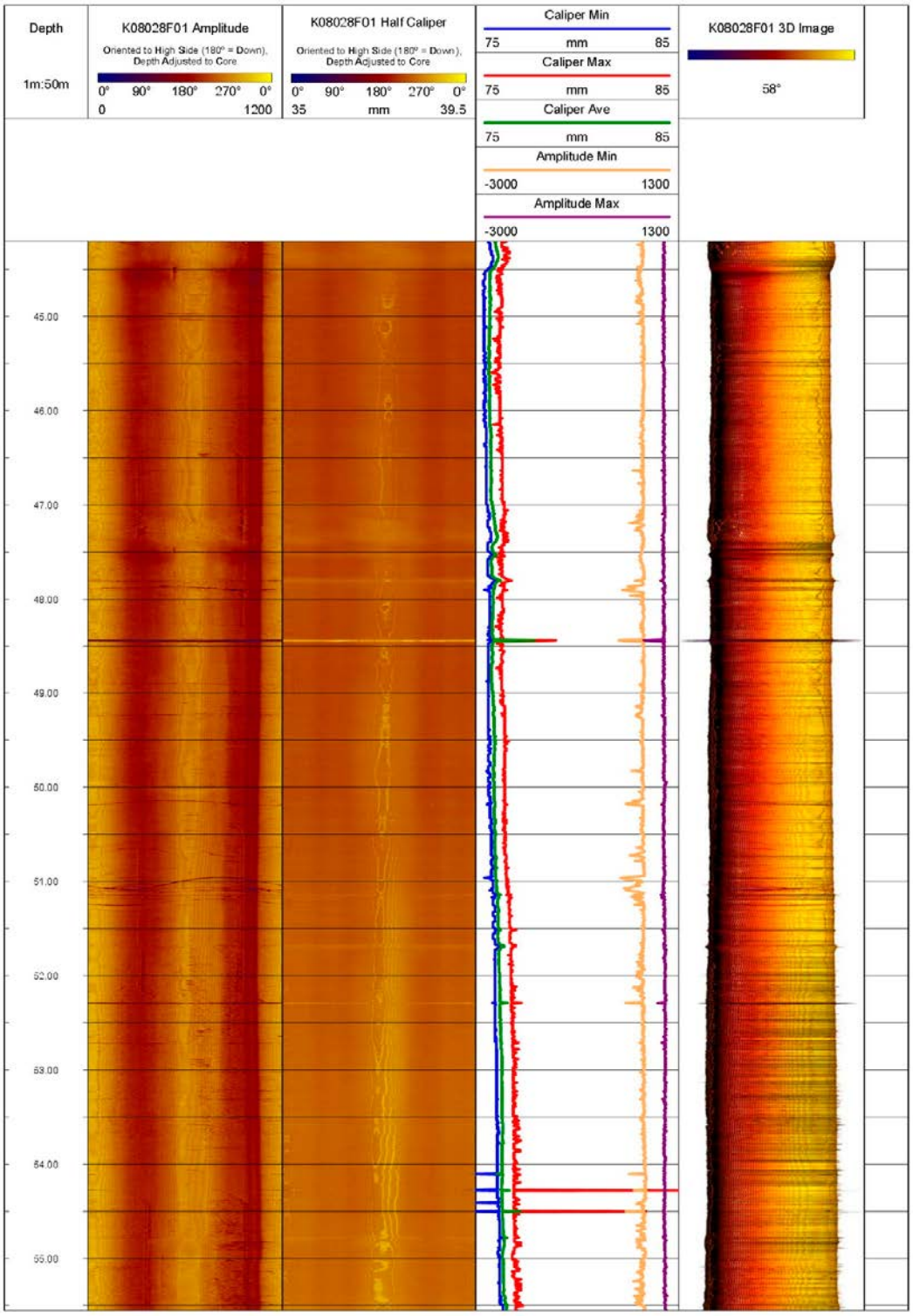
Depth
1m:50m
K08028F01 Amplitude
Oriented to High Side (180° = Down), Depth Adjusted to Core
0° 90° 180° 270° 0°
0
1200
K08028F01 Half Caliper
Oriented to High Side (180° = Down), Depth Adjusted to Core
0° 90° 180° 270° 0°
35
mm
39.5
Caliper Min
75
mm
85
Caliper Max
75
mm
85
Caliper Ave
75
mm
85
Amplitude Min
-3000
1300
Amplitude Max
-3000
1300
K08028F01 3D Image
58°
45.00
46.00
47.00
48.00
49.00
50.00
51.00
52.00
53.00
54.00
55.00

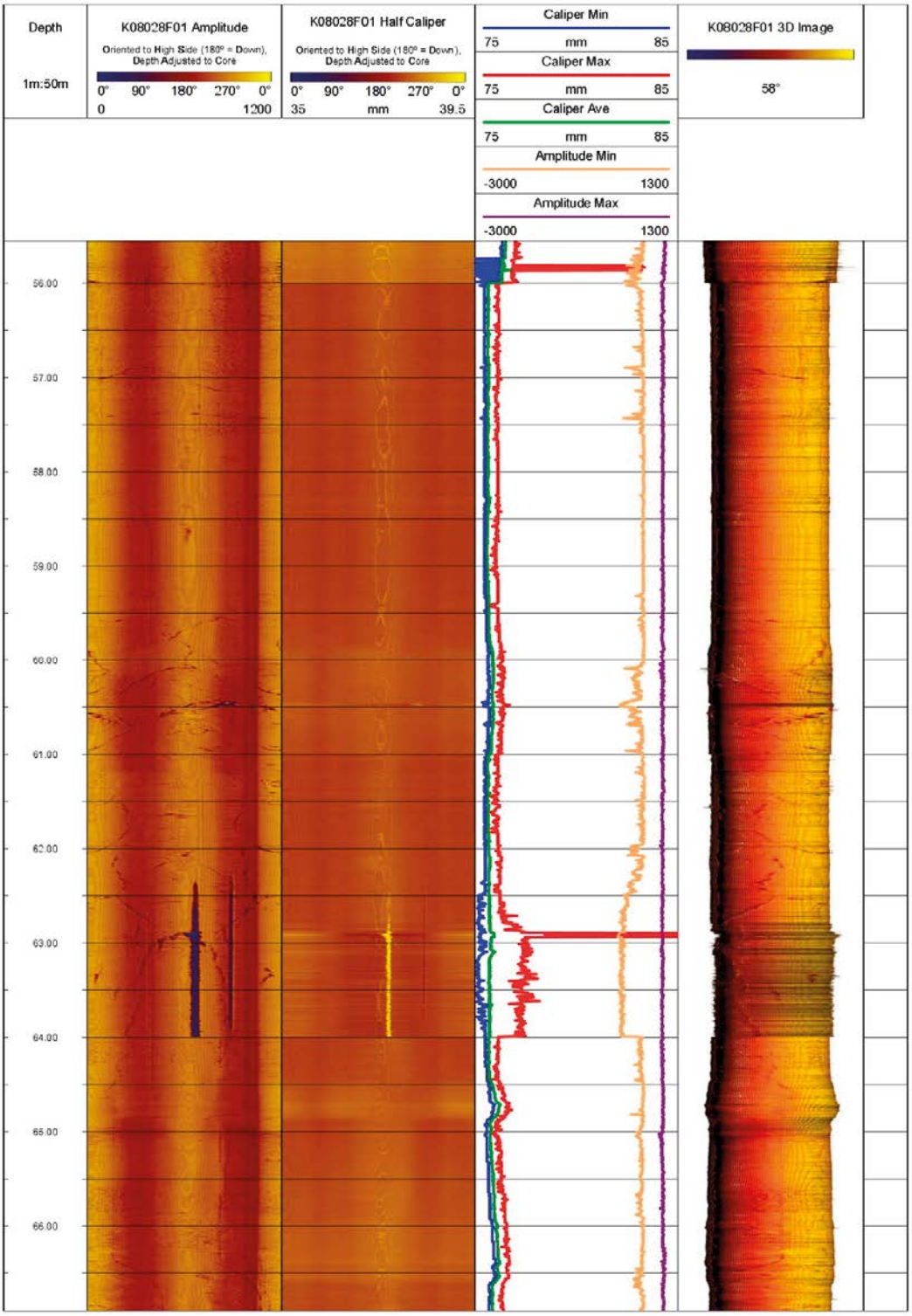
Depth
1m:50m
K08028F01 Amplitude
Oriented to High Side (180° = Down), Depth Adjusted to Core
0° 90° 180° 270° 0°
0
1200
K08028F01 Half Caliper
Oriented to High Side (180° = Down), Depth Adjusted to Core
0° 90° 180° 270° 0°
35
mm
39.5
Caliper Min
75
mm
85
Caliper Max
75
mm
85
Caliper Ave
75
mm
85
Amplitude Min
-3000
1300
Amplitude Max
-3000
1300
K08028F01 3D Image
58°
56.00
57.00
58.00
59.00
60.00
61.00
62.00
63.00
64.00
65.00
66.00

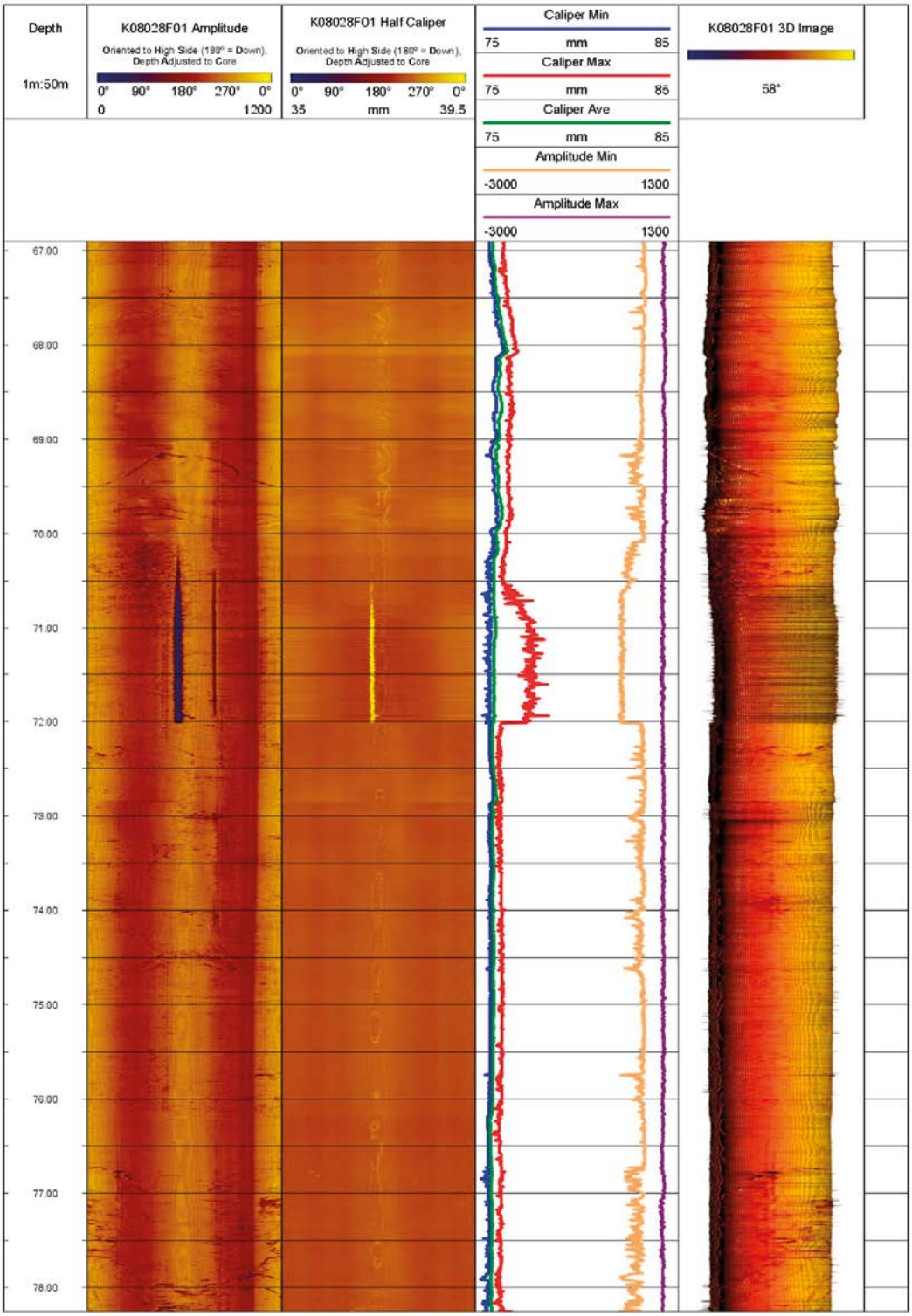
Depth
1m:50m
K08028F01 Amplitude
Oriented to High Side (180° = Down), Depth Adjusted to Core
0° 90° 180° 270° 0°
0
1200
K08028F01 Half Caliper
Oriented to High Side (180° = Down), Depth Adjusted to Core
0° 90° 180° 270° 0°
35
mm
39.5
Caliper Min
75
mm
85
Caliper Max
75
mm
85
Caliper Ave
75
mm
85
Amplitude Min
-3000
1300
Amplitude Max
-3000
1300
K08028F01 3D Image
58°
67.00
68.00
69.00
70.00
71.00
72.00
73.00
74.00
75.00
76.00
77.00
78.00

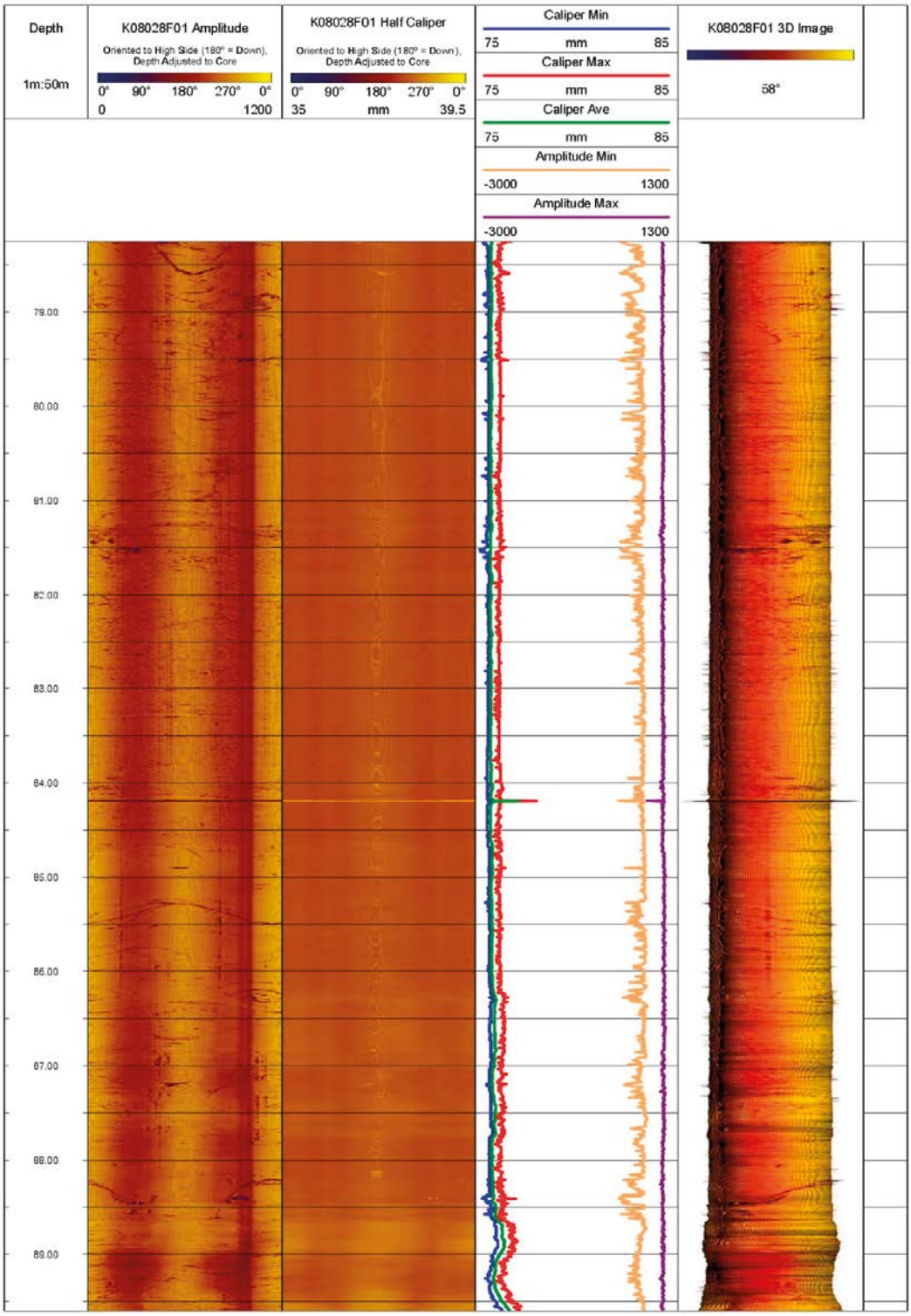
Depth
1m:50m
K08028F01 Amplitude
Oriented to High Side (180° = Down), Depth Adjusted to Core
0° 90° 180° 270° 0°
0 1200
K08028F01 Half Caliper
Oriented to High Side (180° = Down), Depth Adjusted to Core
0° 90° 180° 270° 0°
35 mm 39.5
Caliper Min
75 mm 85
Caliper Max
75 mm 85
Caliper Ave
75 mm 85
Amplitude Min
-3000 1300
Amplitude Max
-3000 1300
K08028F01 3D Image
58°
79.00
80.00
81.00
82.00
83.00
84.00
85.00
86.00
87.00
88.00
89.00

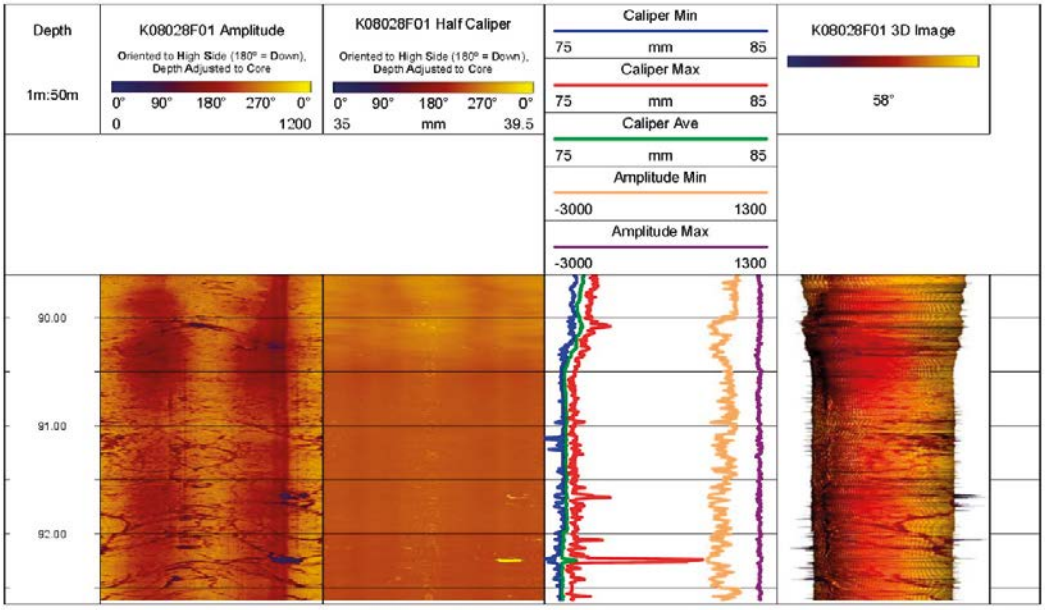
Depth
1m:50m
K08028F01 Amplitude
Oriented to High Side (180° = Down), Depth Adjusted to Core
0° 90° 180° 270° 0°
0
1200
K08028F01 Half Caliper
Oriented to High Side (180° = Down), Depth Adjusted to Core
0° 90° 180° 270° 0°
35
mm
39.5
Caliper Min
75
mm
85
Caliper Max
75
mm
85
Caliper Ave
75
mm
85
Amplitude Min
-3000
1300
Amplitude Max
-3000
1300
K08028F01 3D Image
58°
90.00
91.00
92.00

Rock Mechanical Properties

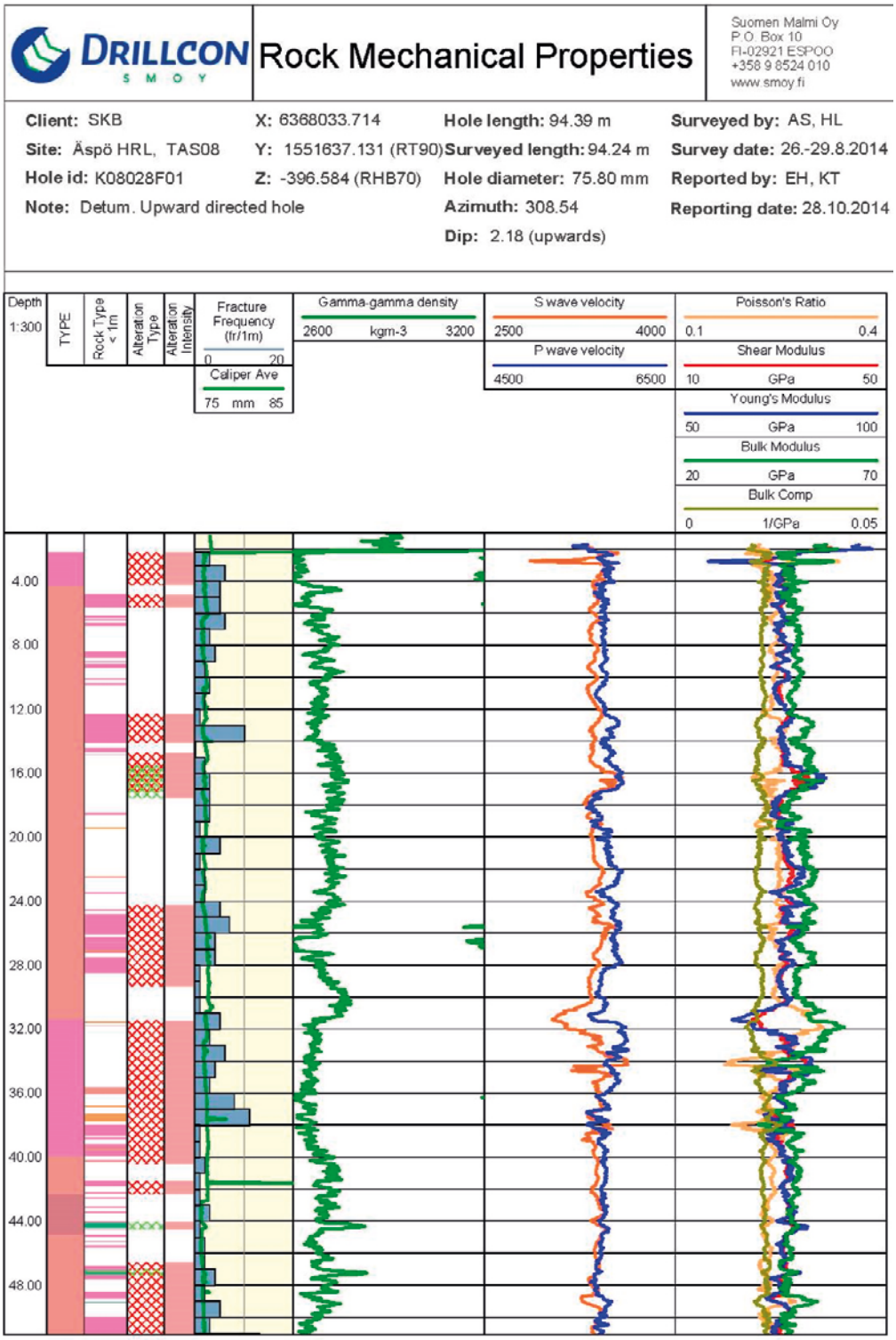

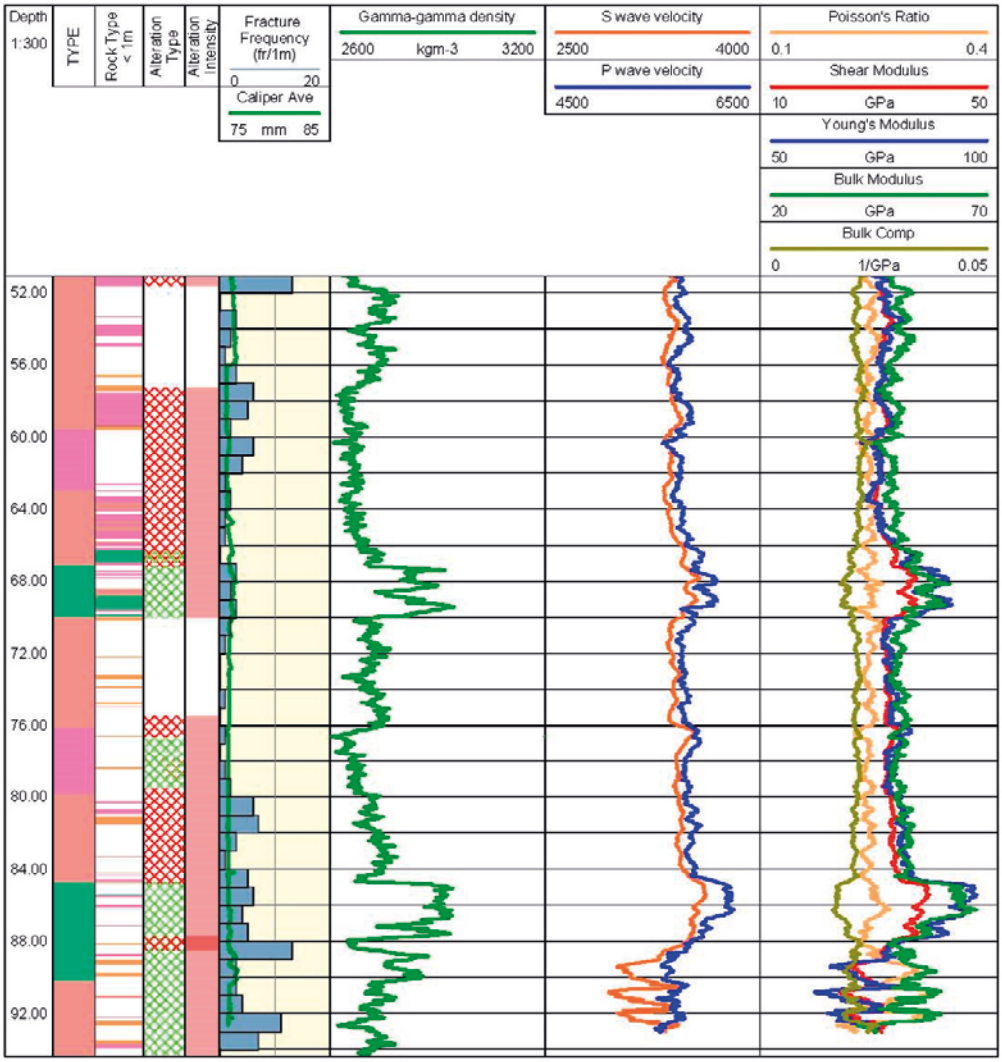
Depth
1:300
TYPE
Rock Type < 1m
Alteration Type
Alteration Intensity
Fracture Frequency (fr/1m)
0 20
Caliper Ave
75 mm 85
Gamma-gamma density
2600 kgm-3 3200
S wave velocity
2500 4000
P wave velocity
4500 6500
Poisson's Ratio
0.1 0.4
Shear Modulus
10 GPa 50
Young's Modulus
50 GPa 100
Bulk Modulus
20 GPa 70
Bulk Comp
0 1/GPa 0.05
52.00
56.00
60.00
64.00
68.00
72.00
76.00
80.00
84.00
88.00
92.00

Full Waveform Sonic

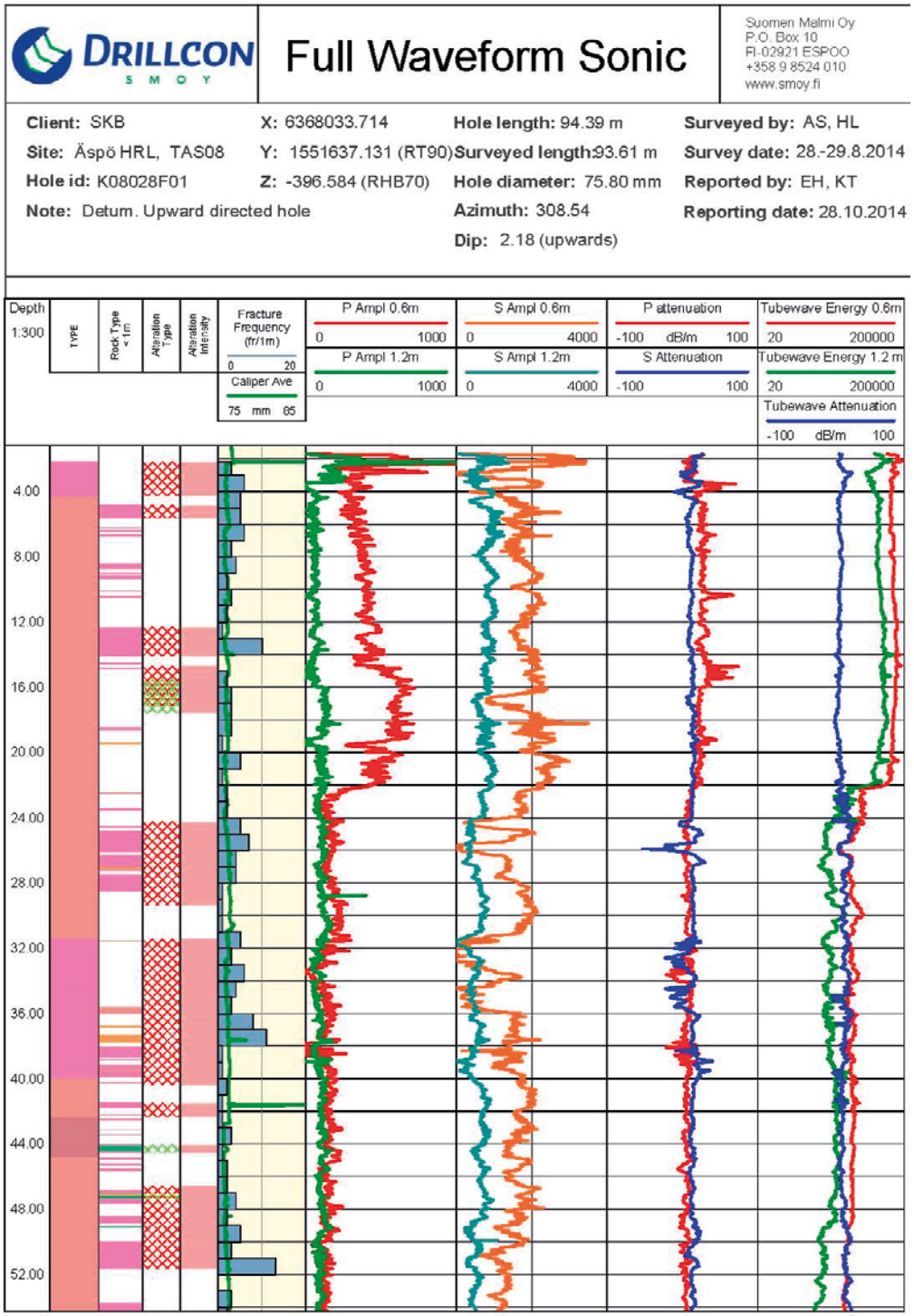

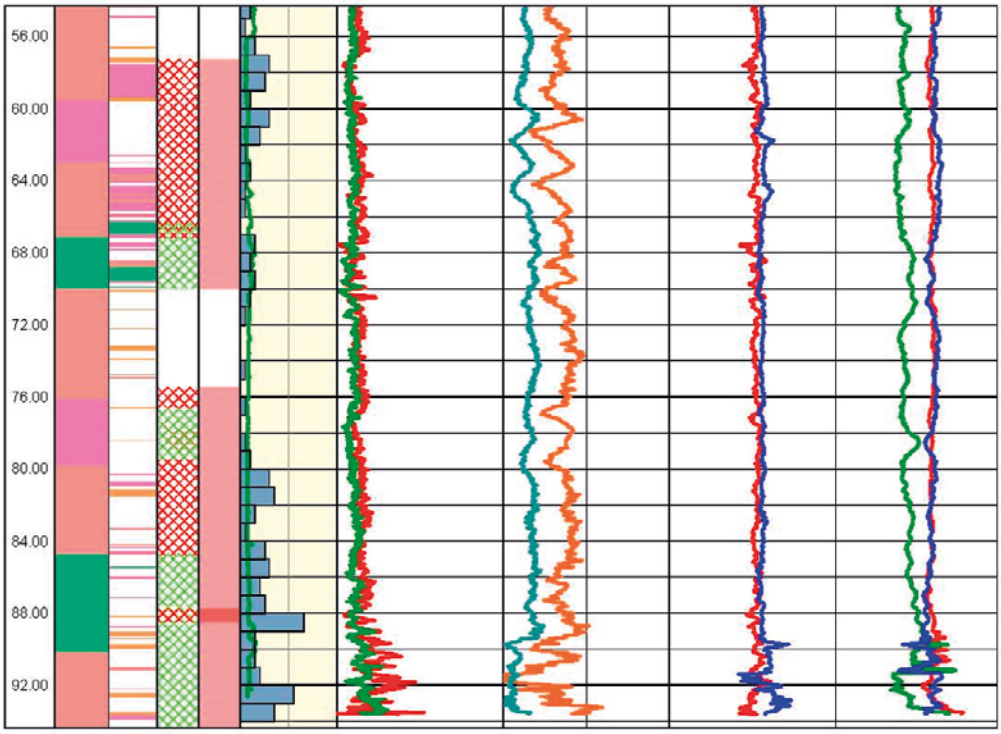
56.00
60.00
64.00
68.00
72.00
76.00
80.00
84.00
88.00
92.00

Full Waveform Sonic, wideband log

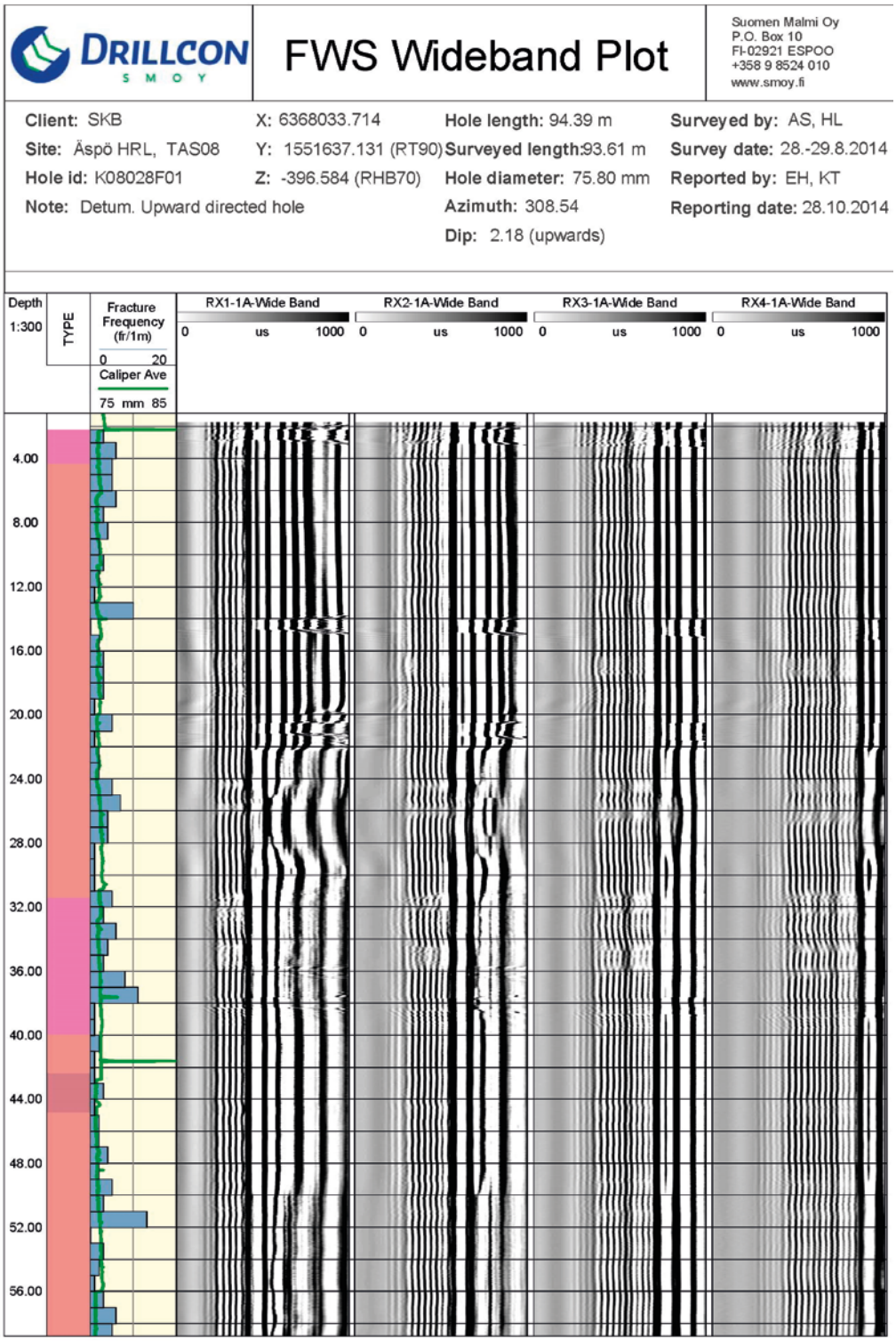

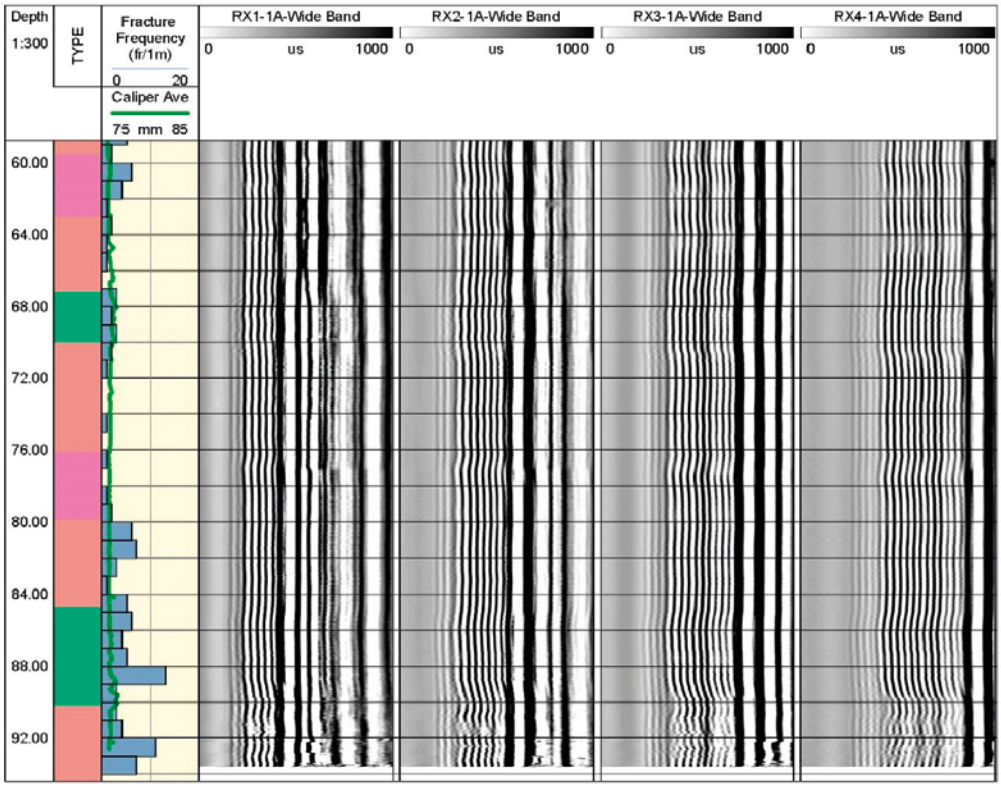
Depth
1:300
TYPE
Fracture
Frequency
(fr/1m)
0 20
Caliper Ave
75 mm 85
RX1-1A-Wide Band
RX2-1A-Wide Band
RX3-1A-Wide Band
RX4-1A-Wide Band
0 us 1000
60.00
64.00
68.00
72.00
76.00
80.00
84.00
88.00
92.00

Full Waveform Sonic, chevron plot

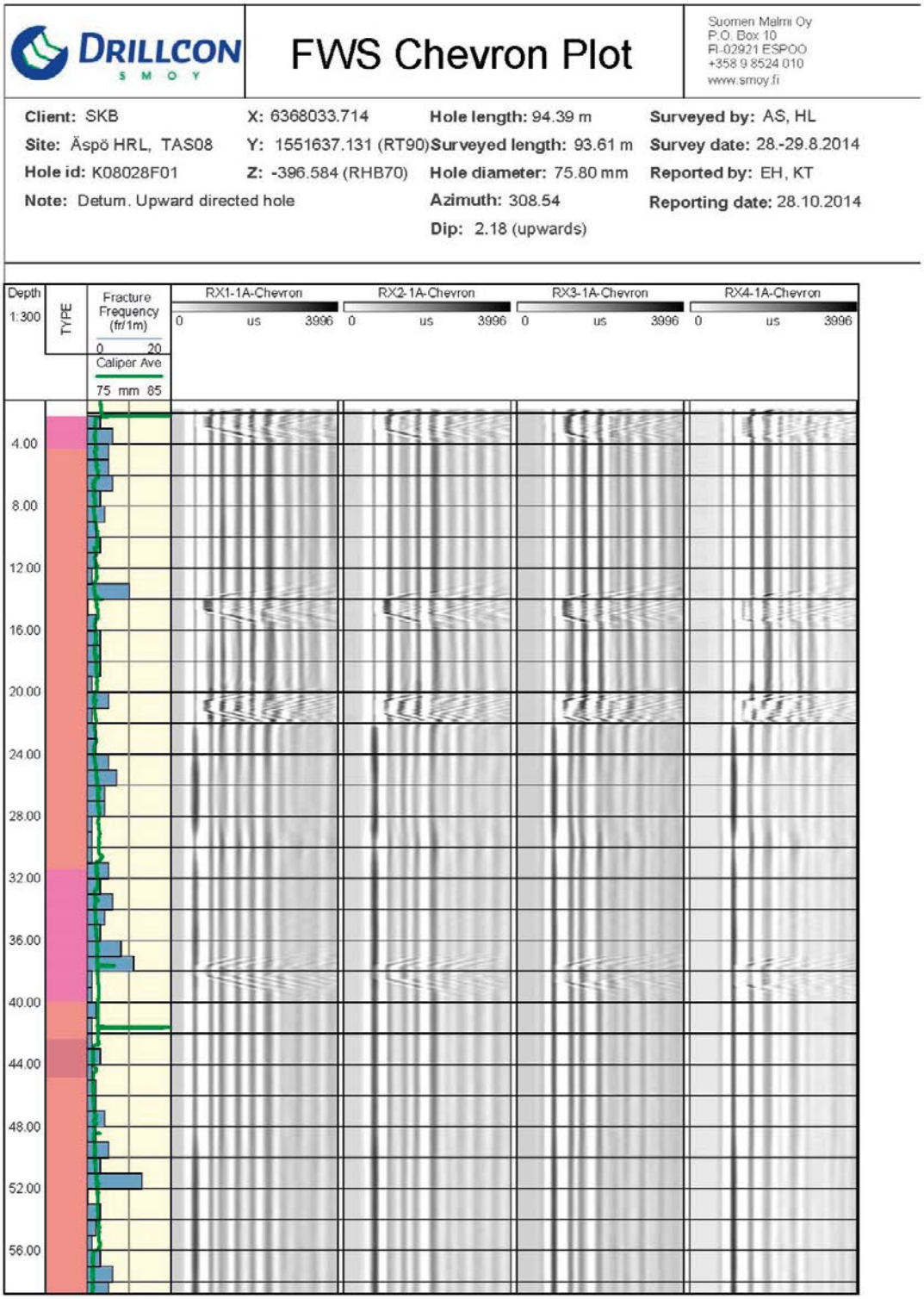

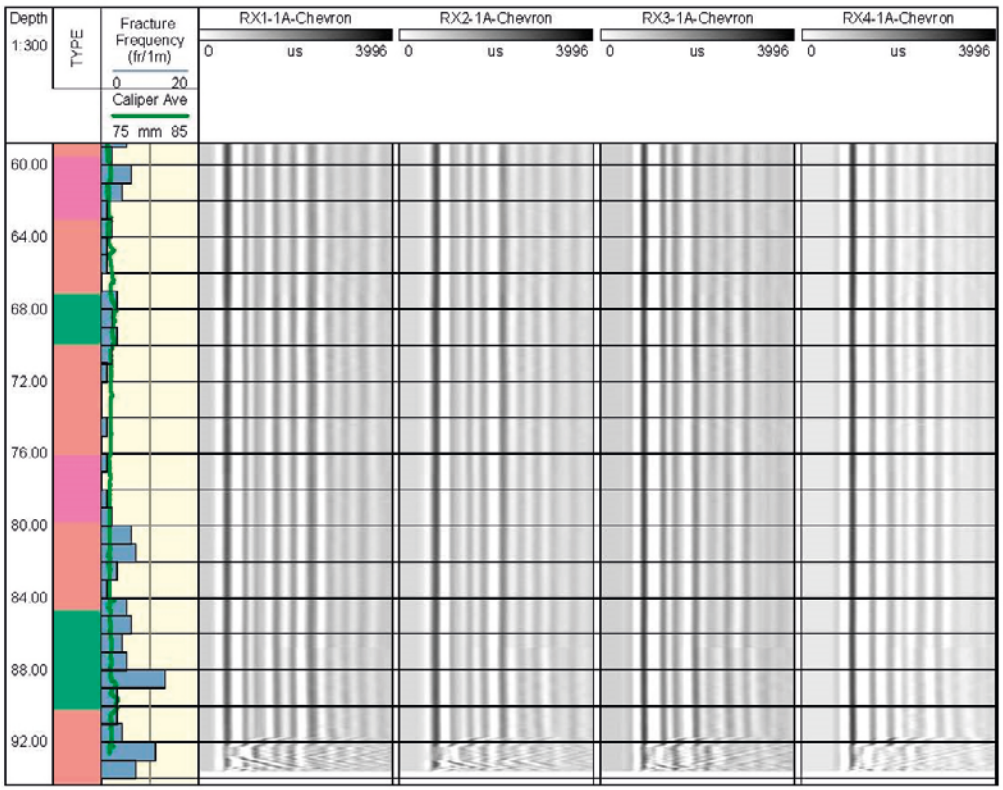
Depth
1:300
TYPE
Fracture Frequency (fr/1m)
0 20
Caliper Ave
75 mm 85
RX1-1A-Chevron
RX2-1A-Chevron
RX3-1A-Chevron
RX4-1A-Chevron
0 us 3996
60.00
64.00
68.00
72.00
76.00
80.00
84.00
88.00
92.00

Full Waveform Sonic, tubewave plot

DRILLCON SMOY

FWS Tubewave Plot

Suomen Malmi Oy
P.O. Box 10
FI-02921 ESPOO
+358 9 8524 010
www.smoy.fi

Client: SKB
Site: Äspö HRL, TAS08
Hole id: K08028F01
Note: Detum. Upward directed hole

X: 6368033.714
Y: 1551637.131 (RT90)
Z: -396.584 (RHB70)

Hole length: 94.39 m
Surveyed length: 93.61 m
Hole diameter: 75.80 mm
Azimuth: 308.54
Dip: 2.18 (upwards)

Surveyed by: AS, HL
Survey date: 28.-29.8.2014
Reported by: EH, KT
Reporting date: 28.10.2014

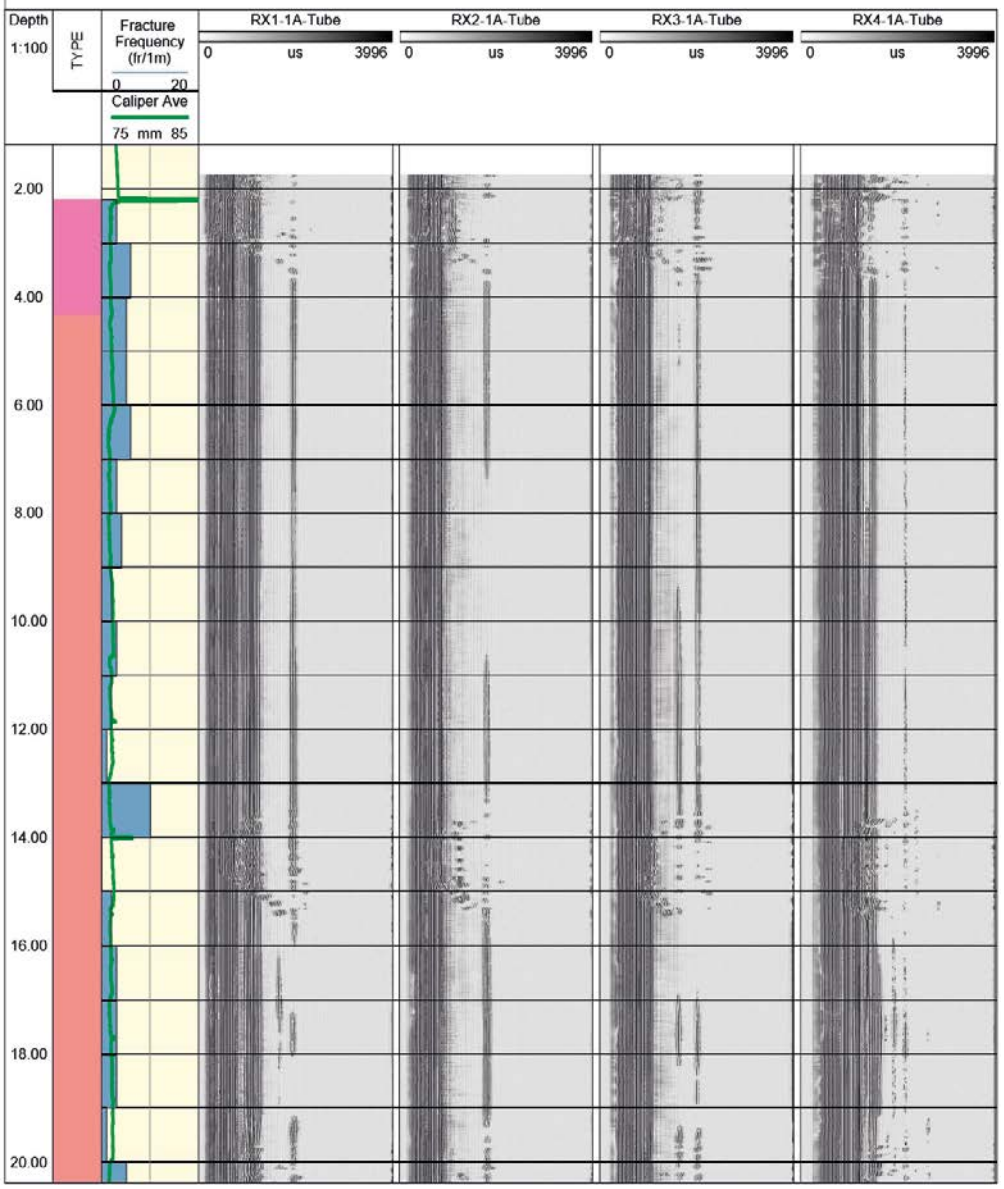

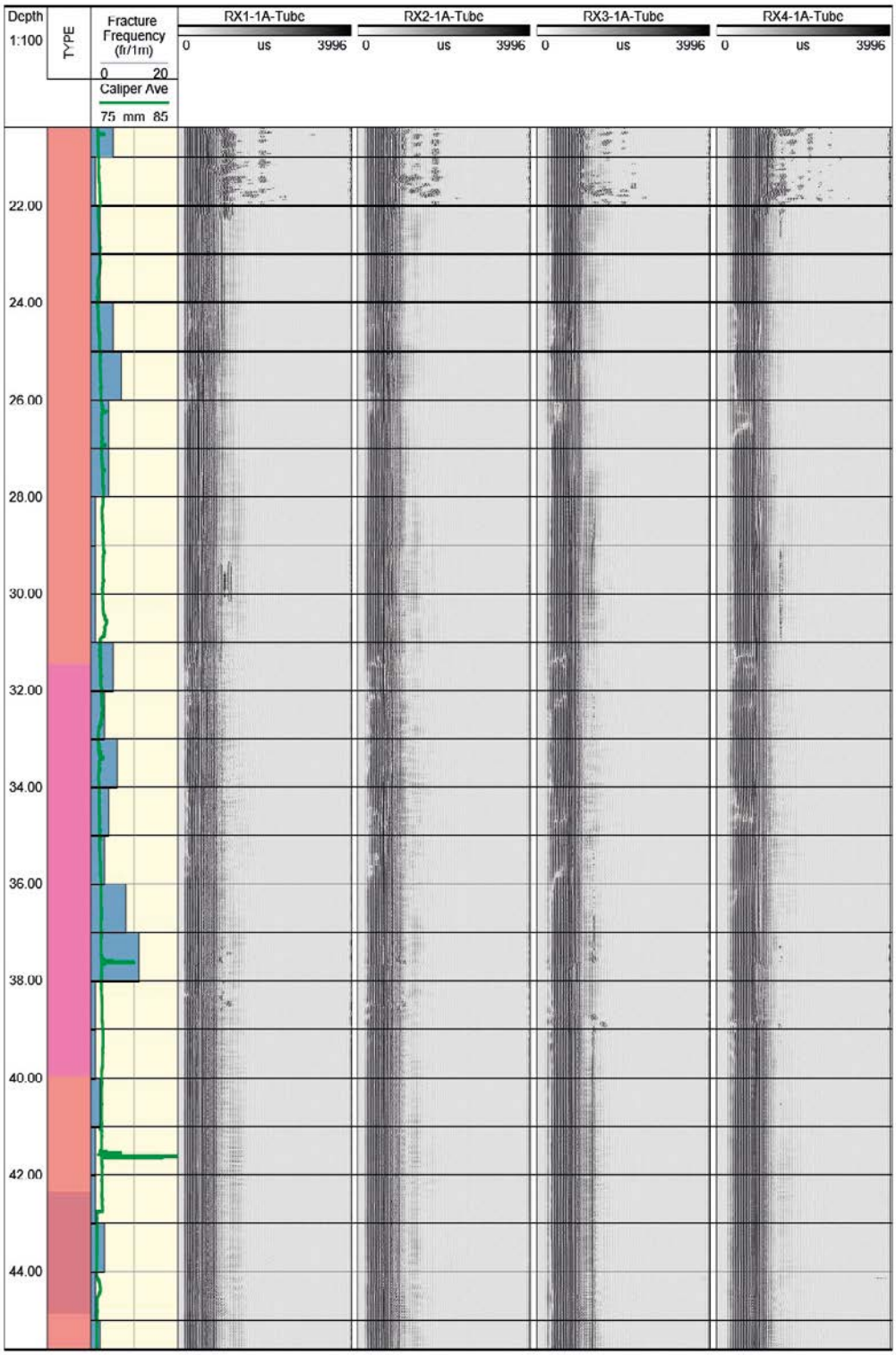
Depth
1:100
TYPE
Fracture Frequency (fr/1m)
0 20
Caliper Ave
75 mm 85
RX1-1A-Tubc
RX2-1A-Tubc
RX3-1A-Tubc
RX4-1A-Tubc
0 us 3996
22.00
24.00
26.00
28.00
30.00
32.00
34.00
36.00
38.00
40.00
42.00
44.00

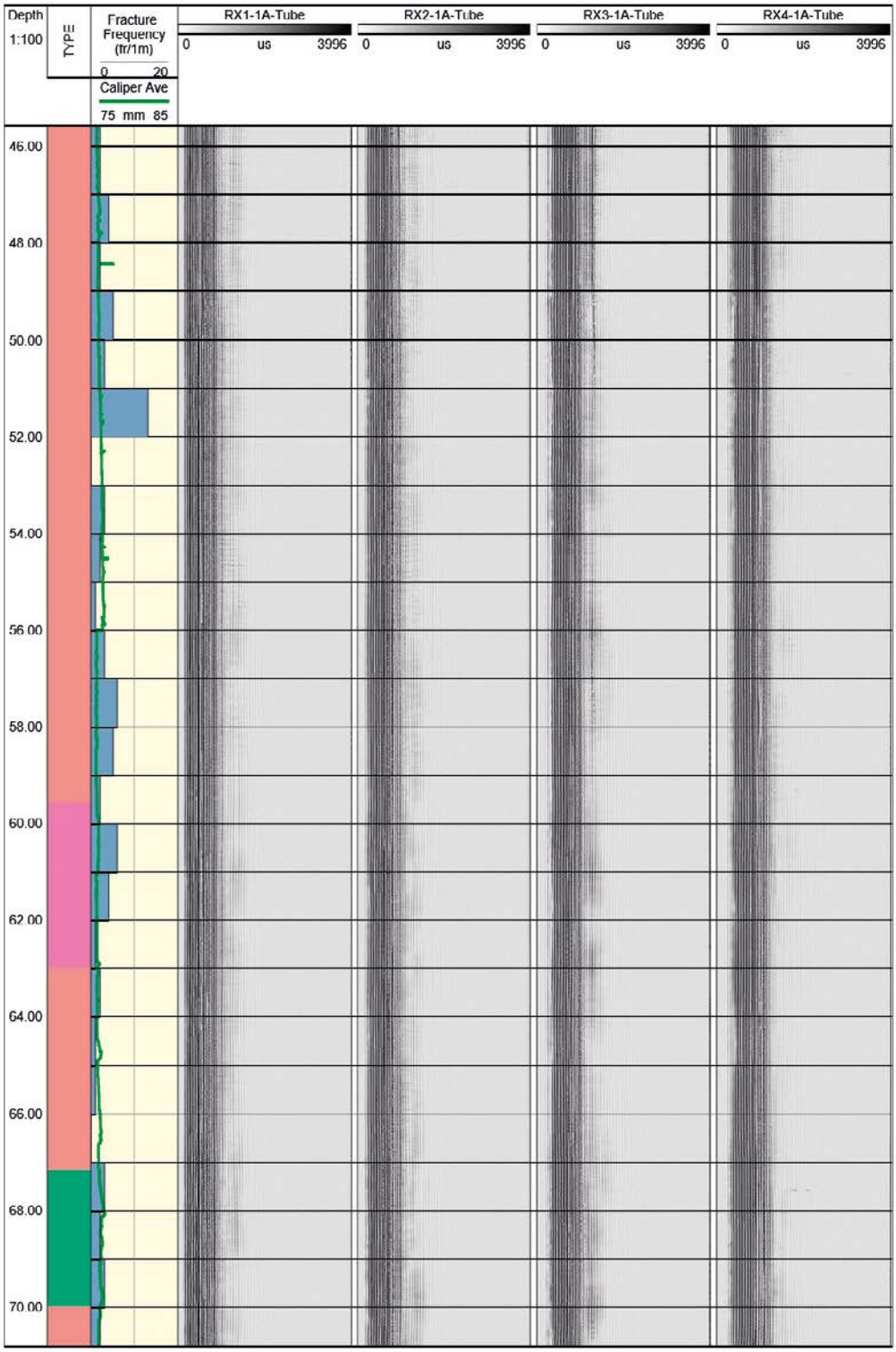
Depth
1:100
TYPE
Fracture Frequency (fr/1m)
0 20
Caliper Ave
75 mm 85
RX1-1A-Tube
RX2-1A-Tube
RX3-1A-Tube
RX4-1A-Tube
0 us 3996
46.00
48.00
50.00
52.00
54.00
56.00
58.00
60.00
62.00
64.00
66.00
68.00
70.00

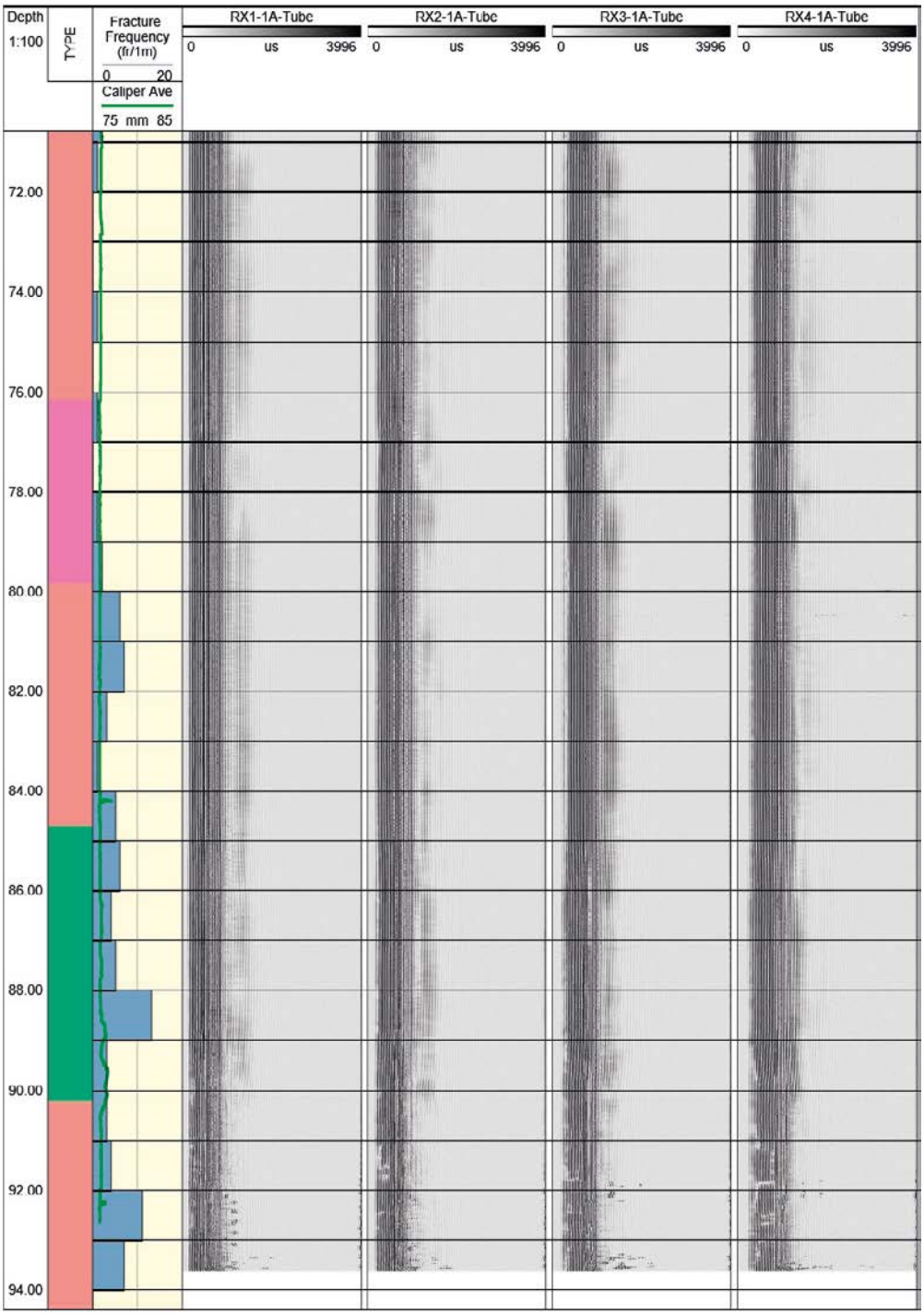
Depth
1:100
TYPE
Fracture Frequency (fr/1m)
0 20
Caliper Ave
75 mm 85
RX1-1A-Tubc
RX2-1A-Tubc
RX3-1A-Tubc
RX4-1A-Tubc
0 us 3996
72.00
74.00
76.00
78.00
80.00
82.00
84.00
86.00
88.00
90.00
92.00
94.00

Arkitektkopia AB, Bromma, 2017

SKB is tasked with managing Swedish nuclear and radioactive waste in a safe way.

skb.se